Tmod2 is a regulator of cocaine responses through control of striatal and cortical excitability, and drug-induced plasticity

Arojit Mitra[1], Sean P. Deats[1], Price E. Dickson[1], Jiuhe Zhu [2], Justin Gardin[1], Brian J. Nieman[3], R. Mark Henkelman[3], Nien-Pei Tsai[2], Elissa J. Chesler[1], Zhong-Wei Zhang[1], Vivek Kumar[1]

[1]The Jackson Laboratory, Bar Harbor, ME, 04609 USA

[2]Department of Molecular and Integrative Physiology, University of Illinois at Urbana-Champaign, Urbana, IL, 61801 USA

[3]Mouse Imaging Centre and Translational Medicine, Hospital for Sick Children; Ontario Institute for Cancer Research; Department of Medical Biophysics, University of Toronto; Toronto, ON, Canada.

Corresponding Author:
Vivek Kumar
The Jackson Laboratory
600 Main St
Bar Harbor, 04609, ME, USA.
+1-207-288-6917
vivek.kumar@jax.org

Abstract

Drugs of abuse induce neuroadaptations, including synaptic plasticity, that are critical for transition to addiction, and genes and pathways that regulate these neuroadaptations are potential therapeutic targets. *Tropomodulin 2* (*Tmod2*) is an actin-regulating gene that plays an important role in synapse maturation and dendritic arborization and has been implicated in substance-abuse and intellectual disability in humans. Here we mine the KOMP2 data and find that *Tmod*2 knockout mice show emotionality phenotypes that are predictive of addiction. Detailed addiction phenotyping showed that *Tmod2* deletion does not affect the acute locomotor response to cocaine administration. However, sensitized locomotor responses are highly attenuated in these knockouts, indicating a potential lack of necessary drug-induced plasticity. In addition, *Tmod2* mutant animals do not self-administer cocaine indicating lack of hedonic responses to cocaine. Whole brain MR imaging shows differences in brain volume across multiple regions although transcriptomic experiments did not reveal perturbations in gene co-expression networks. Detailed electrophysiological characterization of *Tmod2* KO neurons, showed increased spontaneous firing rate of early postnatal and adult cortical and striatal neurons. Cocaine-induced synaptic plasticity that is critical for sensitization is either missing or reciprocal in *Tmod2* KO nucleus accumbens shell medium spiny neurons, providing a mechanistic explanation of the cocaine response phenotypes. Combined, these data provide compelling evidence that *Tmod2* is a major regulator of plasticity in the mesolimbic system and regulates the reinforcing and addictive properties of cocaine.

Introduction

Multiple lines of evidence suggest that enduring functional and structural plasticity in reward-related brain regions are critical for transition to addiction[1, 2]. Although the entire brain reward circuit is vulnerable to drug-induced functional and structural remodeling[3], it is relatively well characterized in nucleus accumbens. Functional plasticity broadly refers to changes in intrinsic and synaptic properties of existing synapses whereas structural plasticity includes morphological changes such as dendritic spine class and density alterations[4]. Drug-induced functional plasticity in nucleus accumbens includes changes in intrinsic properties such as firing rate depression, or synaptic changes such as AMPAR-mediated long-term depression[5, 6]. These plasticity events have been shown to facilitate initiation and maintenance of reward-related behaviors[5-10].

Along with functional plasticity, repeated drug administration is also thought to facilitate structural plasticity in the mesolimbic circuit. Repeated administration of psychostimulants correlates with increased spine density and dendritic complexity in the nucleus accumbens, ventral tegmental area, and prefrontal cortex neurons[11]. Dendritic spines are actin-rich protrusions of the neural plasma membrane that are major postsynaptic sites of excitatory signaling in the brain and sub-cellular substrate of synaptic and structural plasticity. Perturbations in actin-assembly[12-16], -capping[17, 18], -disassociating[19, 20], -nucleating[21, 22] and -ADP/ATP exchange[23] proteins affects synaptic and structural plasticity. Previous studies have implicated actin dysregulation in morphine[24], cocaine[25], methamphetamine[26], alcohol[27] and nicotine[28, 29] addiction. Generally, psychostimulant administration correlates with increases in spine numbers, spine complexity, and spine maturity[30-32]. These structural changes occur through actin-mediated rearrangements[20, 22]. Consistent with these observations, non-muscle myosin IIB inhibitor, which mitigates spine maturation by inhibiting crosslinking and treadmilling of F-actin, has been shown effective in preventing relapse to methamphetamine[33]. Our previous study demonstrated that a point mutation in actin-regulating cytoplasmic FMRP interacting protein-2 (*Cyfip2*) in mice decreases both acute and sensitized cocaine responses[21]. However, a causal link between structural changes and behavioral effects of repeated exposure to drugs remains controversial[2]. Genetic or pharmacological

perturbations of factors that are known to regulate structural plasticity, such as kalirin-7, myocyte enhancer factor-2, and cyclin-dependent kinase-5, fail to attenuate behavioral locomotor sensitization in mice[31, 34-36]. Thus, the possibility has been raised that structural plasticity in transition to addiction is an "epiphenomenon"[2].

The neuron-specific, tropomyosin-dependent pointed end capping protein tropomodulin-2 (TMOD2), stabilizes actin filament by preventing depolymerization and elongation[37]. Four isoforms of tropomodulin (*Tmod1-4*) are expressed with tissue specificity in mice. *Tmod1* and *Tmod3* are ubiquitously expressed, whereas *Tmod4* and *Tmod2* are restricted to muscle and neurons, respectively[38]. Previous studies have established a role for TMOD2 in dendritic arborization[39] and spine maturation[40]. During development, its expression coincides with generation, migration, and extension of cerebrum and cerebellum neurons during the prenatal period[41, 42]. In addition to pointed end capping of actin filament, an *in vitro* protein interaction study shows actin-monomer binding and strong actin-nucleation activity by TMOD2[43].

Tmod2 knockout mice exhibit novelty-induced hyperactivity, memory deficits in a fear conditioning task and enhanced long term potentiation at hippocampal synapses[17]. Recent human GWAS studies have shown that *Tmod2* haplotypes are associated with cognitive impairments[44, 45]. In human candidate gene studies, Gelernter and colleagues showed that *Tmod2* is associated with drug-dependent risk-taking behavior and proposed TMOD2-mediated remodeling of brain areas regulating sexual function and behavior[46]. In several transcriptomics and proteomics studies, *Tmod2* mRNA and protein levels are differentially modulated following repeated methamphetamine[47-49], alcohol[50], cocaine[51], or morphine[52] administration in animal models. These studies led a meta-analysis to suggest *Tmod2* is an addiction candidate gene[53]. However, to date, there has not been a study that directly investigates a causal role of *Tmod2* in addiction phenotypes and provides mechanistic insights into its function in the reward circuit.

Based on previous human genetic data and KOMP emotionality phenotype data, we hypothesized that *Tmod2* is a regulator of addiction phenotypes. To test this we carried out detailed addiction characterization for cocaine responses and find that sensitized response and intravenous self-

administration (IVSA) acquisition are diminished in *Tmod2* knockout mice. Imaging and genomics data show reduced brain size but no major perturbances in gene co-expression networks. Finally, a detailed characterization of the intrinsic properties of cortical and striatal neurons at postnatal and adult stages show enhanced excitability. Synaptic events that are hallmarks of cocaine-induced synaptic plasticity in the nucleus accumbens medium spiny neurons are missing in the knockouts. Together, our data provide compelling evidence that the actin-regulating gene *Tmod2* plays a critical role in cocaine-induced behavioral adaptations that are critical for transition to addiction.

Experimental procedures

Animals and drugs

Tropomodulin 2 (*Tmod2*$^{-/-}$) knockout mice, B6N(Cg)-*Tmod2*$^{tm1b(KOMP)Wtsi}$/2J (JR# 024939; referred to as *Tmod2* KO in text or KO in figures) with a LacZ reporter gene and C57BL/6NJ (JR# 005304; control referred to as WT) mice were obtained from The Jackson Laboratory, Bar Harbor. Both male and female mice were used for experiments. Mice were bred for at least two generations in an in-house colony before experimentation. Animal handling and experimental procedures were approved by Institutional Animal Care and Use Committees at The Jackson Laboratory. Cocaine hydrochloride (CAS no. 53-21-4, Sigma) was dissolved in 0.9% NaCl (vehicle) and was administered intraperitoneally.

Data mining from KOMP repository

Data generated by The Jackson Laboratory's KOMP phenotyping pipeline on *Tmod2* KO mice were harvested from International Mouse Phenotyping Consortium website and is publically available at http://www.mousephenotype.org/data/genes/MGI:1355335#section-associations. Details of the phenotyping pipeline, behavioral assays and parameters are available at http://www.mousephenotype.org/impress/procedures/7.

Locomotor response to acute injection of cocaine

All testing was carried out between Zeitgeber time 3 and 11 (ZT 3-11). Mice were habituated to handling and testing room conditions prior to behavioral assays. Mice (10 weeks old) were brought into the testing room and habituated to the open field testing room for 1 hour with white noise (75 ± 2 decibels), before introducing them to the open field. Locomotor activity was recorded using an overhead camera and Limelight software (Actimetrics, Wilmette, IL) before and after the injections. One single dose of low (10 mg/kg) or high (20 mg/kg) dose of cocaine was injected and the locomotor activity was recorded for 1 h[54].

Locomotor sensitization

Following 1 h habituation to testing room, mice (10 weeks old) were introduced in an open field arena and locomotor activity before and after the saline or cocaine injections were recorded. Mice received saline for 4 days and cocaine (15 mg/kg) for the next 6 days followed by 1 saline injection on day 11. A same-dose cocaine challenge on day 17 and an additional challenge on day 24 were given (see timeline in fig 2D)[54].

Intravenous self-administration (IVSA) assay

The cocaine IVSA testing procedure and chambers have been described in detail previously[55]. Mice began cocaine IVSA testing on a fixed-ratio 1 schedule at a dose of 1.0 mg/kg/infusion. Mice were tested in two-hour sessions at the same time daily seven days per week throughout the experiment. Acquisition criteria were defined as (a) ≥ 10 infusions per session on 3 consecutive or non-consecutive sessions followed by (b) 2 consecutive sessions during which number of infusions was ≥ 10, did not vary by more than 20%, and ≥ 70% of lever presses were on the active lever .

Sucrose Preference

Mice were singly housed for this protocol in a cage with the metal roof lid having inserts for 2-3 bottles and access to *ad libitum* chow. Baseline water consumption was assessed by providing water in 2 bottles for 4 consecutive days and measuring bottle weight in 24 h interval. At the end of 4th day, one of the bottles is filled with freshly prepared 4% sucrose solution and consumption was assessed for the next 4 days. The position of bottles were changed daily to avoid any physical preference or side bias towards the bottle. The bedding below the sipper bottles was monitored daily to account for spillage. If the bedding was found moist or wet with an unusual quantity of consumption for a day, the intake data was not included in the analysis. Preference is calculated as the percentage of the sucrose consumed over the total volume of fluid intake on day 8[56].

Operant Conditioning for food reward

9-week old mice were subjected to mild food restriction to maintain 80-90% of *ad libitum* body weight during the entire 15 days of the protocol. Mice were habituated to the operant chamber (Med Associates, Inc., Fairfax, VT) for 30 min for 2-3 days with house light and fan on and levers retracted. Following habituation, levers were made accessible and the active lever press was associated with a delivery of one (FR1) 15mg sucrose pellet (#S05550; Bio-serv, Flemington, NJ) as a reward and a time-out period of 20 s during which the house light is switched off. Inactive lever press was not associated with any reward or observable stimuli. Daily 1 h sessions were provided at the same time of the day, for 10 days. Total number of sucrose pellets earned, and the number of active and inactive lever press were recorded and statistically compared between *Tmod2* KO and WT. On the subsequent 5 days (day 11-15), an extinction paradigm was introduced where active lever press yielded no reward and the house light stays on for the entirety of the session. On day 16, a reinstatement session was provided, with conditions similar to the acquisition phase during day 1-10.

Magnetic resonance imaging

10-week old *Tmod2* KO (n=15) and WT (n=19) were deeply anesthetized and transcardially perfused with 30 ml, 1X PBS with 1 µl/ml heparin and 2mM ProHance (Bracco Diagnostics, Princeton, NJ) at room temperature, at a flow rate of 1 ml/min. Fixation, storage, and imaging procedures have been described in detail previously[57, 58]. For this study, T_2-weighted RARE images were acquired on a 7-T scanner (Varian/Agilent) with imaging parameters: TE_{eff}=30ms, TR=350ms, 6 echoes, 4 averages, 40µm resolution, 13hour scan time. The resulting images were analyzed using an automated registration pipeline[59] in conjunction with predefined structural atlases[60]. The resulting images obtained were analyzed for total brain, total gray matter and total white matter volume differences. Regional differences in structure were assessed through two different methods. In the first, we measured (absolute) volumes for each structure to evaluate the differences between genotypes, fitting with a linear model with sex, genotype and sex-genotype interaction coefficients. Significance was determined after correction for

multiple comparisons through the false discovery rate (and expressed as q values)[61]. In a second analysis, individual structure volumes were normalized to total brain volume so that each structure was evaluated as a percentage of total brain volume. The second approach accounts for a significant amount of the biological variability between mice[62].

Bulk RNA sequencing

Naïve, 10-week old *Tmod2* KO (n=3) and WT (n=3) mice were euthanized by cervical dislocation and the brains were harvested rapidly in ice-cold 1X PBS. 1 mm thick coronal sections were obtained using stainless steel brain matrix (Stoelting, Wood Dale, IL) and punches were taken from primary and secondary motor cortices, and striatum. The punchers were immediately transferred in 1.5 ml tubes containing 250 µl of RNA*later* (#AM7020, Invitrogen) and stored at 4˚C, overnight. Next day, these tubes were transferred to -80°C freezer for long-term storage. Tissues were lysed and homogenized in TRIzol Reagent (Ambion), then RNA was isolated using the miRNeasy Mini kit (Qiagen), according to manufacturers' protocols, including the optional DNase digest step. Sample concentration and quality were assessed using the Nanodrop 2000 spectrophotometer (Thermo Scientific) and the RNA 6000 Nano LabChip assay (Agilent Technologies). Libraries were prepared by the Genome Technologies core facility at The Jackson Laboratory using the KAPA mRNA HyperPrep Kit (KAPA Biosystems), according to the manufacturer's instructions. Briefly, the protocol entails isolation of polyA containing mRNA using oligo-dT magnetic beads, RNA fragmentation, first and second strand cDNA synthesis, ligation of Illumina-specific adapters containing a unique barcode sequence for each library, and PCR amplification. Libraries were checked for quality and concentration using the D5000 ScreenTape assay (Agilent Technologies) and quantitative PCR (KAPA Biosystems), according to the manufacturers' instructions. For sequencing, libraries were pooled and sequenced by the Genome Technologies core facility at The Jackson Laboratory, 75 bp single-end on the NextSeq 500 (Illumina) using NextSeq High Output Kit v2 reagents (Illumina).

Electrophysiology

Microelectrode array (MEA) recordings on primary cortical neuron culture

Primary cortical neuron cultures were made from mice P0-P1 as described previously[63]. Briefly, pups at P0-P1 (n=4, *Tmod2* KO; n=6, WT) were anesthetized on a cold metallic block placed on a bed of ice. Brains were taken out and the entire cortical region was micro-dissected in an aseptic environment (a bio-chemical hood). Cortical tissues were immediately transferred to ice cold hibernate AB complete media (BrainBits, Springfield, IL) and were shipped to collaborators at University of Illinois at Urbana-Champaign, Urbana, IL, USA. Details of cell dissociation, maintenance on MEA plates, recordings, parameters analyzed and compared was described previously[64]. Briefly, on DIV 15, MEA plates were placed inside the recording chamber with inbuilt humidifier, and access to 5% CO_2 at 37˚C. 15 min baseline recording were obtained before application of pharmacological agents such as GABA-A receptor blocker picrotoxin (PTX) and AMPA receptor antagonist NBQX. For analysis, 10 min baseline spiking activity before drug application was compared with 10 min response window following 5 min of drug application (Fig 4B). Fold change in spontaneous spike rate, burst number and synchrony index is a ratio of response and baseline periods. Fold change of 1 represents no change, >1 represent response value of the parameter was more than baseline and <1 represents a decrease in response value.

Intrinsic properties of cortical and striatal neurons

Mice were deeply anesthetized using 4% tribromoethonol (800mg/kg), decapitated and the brain was quickly dissected out in ice-cold solution containing (in mM): 210 sucrose, 26 $NaHCO_3$, 10 glucose, 3 KCl, 4 $MgCl_2$, and 1 $CaCl_2$ aerated with 95% O_2 and 5% CO_2. Using a vibratome (Leica VT1200) 250 µm brain slices from naïve, 8-week old *Tmod2* KO (n=6) and WT (n=6) mice were obtained containing pre-limbic area (coronal sections) of the medial prefrontal cortex or accumbens shell (sagittal sections). Slices were then transferred to a holding chamber with artificial cerebrospinal fluid (ACSF) at room temperature containing (in mM): 124 NaCl, 3.0 KCl, 1.5 $CaCl_2$, 1.3 $MgCl_2$, 1.0 NaH_2PO_4, 26 $NaHCO_3$, and 20 glucose; saturated with 95% O_2 and 5% CO_2 at room temperature (21–24°C). Slices were incubated for at

least 1 h for neurons to recover and equilibrate to the ACSF, before performing the whole-cell recordings. For recordings, slices were transferred to a submersion-type chamber attached to a microscope and were continuously perfused with ACSF saturated with 95% O_2 and 5% CO_2 at 30-32˚C. Pyramidal cells of the prelimbic cortex and medium spiny neurons in accumbens shell were identified using 40X objective. Medium spiny neurons were additionally screened by their low resting membrane potential of -75 mV or lower. Whole-cell recordings were obtained from neuron cell bodies using MultiClamp 700B amplifier (Molecular Devices, Sunnyvale, CA, United States) and glass pipette containing (in mM): 120 K-gluconate, 20 KCl, 10 HEPES, 0.2 EGTA, 2 $MgCl_2$, and ATP/GTP (pH 7.2-7.3). Series resistance was fully compensated in current clamp mode. All the protocols were made and executed through the AxoGraph X software (AxoGraph Scientific). Data were filtered at 4 kHz and digitized at 20 kHz. Data analysis was performed using AxoGraph X.

Intrinsic properties of neurons were analyzed using methods described previously[65, 66]. Resting membrane potentials were measured within 20 s of break-in. Input resistance, time constant and whole-cell capacitance were calculated from voltage responses to 700 ms current steps of -40 pA. To compensate for changes in resting membrane potential, cells in prelimbic cortex and accumbens shell were held at -70 and -80 mV, respectively, between current steps.

Synaptic properties of striatal neurons

9-week old *Tmod2* KO (n=6) and WT (n=6) were either injected with saline (n=6, 3 from each strain) or cocaine (15mg/kg; n=6, 3 from each strain), once per day for 5 days. Following injections, mice were transferred to a new cage to facilitate locomotor sensitization[67]. After 3-8 days of abstinence, mice were sacrificed and sagittal brain sections containing accumbens shell regions were obtained as mentioned above. The recording ACSF contains 0.5 μM tetrodotoxin in addition to the ingredients mentioned earlier. A non-potassium, cesium (Cs) based pipette solution was used containing (in mM): 117 Cs-gluconate, 20.0 HEPES, 0.4 EGTA, 2.8 NaCl, 5.0 tetraethylammonium chloride and 4.0 QX-314 (pH 7.2-7.3). Recordings were performed in voltage-clamp mode and cells were held at -60 mV for recording miniature

excitatory postsynaptic current (mEPSC) and thereafter, at +5 mV for recording miniature inhibitory postsynaptic currents (mIPSC). Amplitude, frequency, rise and decay time of mEPSCs and mIPSCs were analysed using AxoGraph X as described previously[68]..

Results

Addiction-predictive behavior assessment using data in KOMP repository

A large body of literature suggests common underlying neurobiological pathways between addiction traits and other behavioral traits. Behavioral traits such as anxiety, novelty seeking, stress, and impulsivity, are predictive of alcohol- and drug-related phenotypes in humans and rodents. In humans, epidemiological and twin studies show comorbidity between addiction phenotypes and sensation-seeking, impulsivity, and anxiety[69-71]. These human studies are consistent with studies in experimental animals indicating that sensation seeking, novelty preference, and impulsivity predict psychostimulant self-administration[72, 73].

Since KOMP uses metadata splits which can create imbalanced classes of controls and mutants, we reanalyzed the existing data using local controls. We analyzed the *Tmod2* phenotype data present in the public domain through the KOMP repository. Data from *Tmod2* knockout (n=16) and WT mice (C57BL/6NJ; n=68-92) that were tested concurrently ± 3 days were used for all the analyses. We specifically analyzed the results obtained from open field assay (OFA), light-dark box assay (LD), hole board (HB), paired-pulse inhibition test (PPI), and rotarod test (RR). All data are included as supplementary materials (Supplemental Table S1).

Hyperactivity and low anxiety in novel environment

Behavior exhibited in an open field arena measures general locomotor activity, exploratory drive, anxiety-related behavior, and habituation learning. The mice were allowed to explore the open field arena, undisturbed, for 20 min and the activity was statistically compared in four, 5 min bins (Fig 1A1). *Tmod2* KO mice exhibit general hyperactivity that persisted for 20 minutes with a sign of habituation as seen by the bin-to-bin decline in distance traveled in 20 min. *Tmod2* KO mice show persistent hyperactivity compared to WT with increased number of breaks in all four, 5 min bins (Fig 1A1, genotype, $F(1,328)=180$, $p<0.0001$; time-bins, $F(3,328)=22.43$, $p<0.0001$; genotype X time-bins, $F(3,328)=10.05$, $p<0.0001$). Consequently, total time spent mobile was also significantly elevated in *Tmod2* KO (Fig 1A5,

t=7.973, p<0.0001). *Tmod2* KO spends more time in the center (Fig 1A3, t=6.662, p<0.0001) and exhibited increased percent locomotor activity in the center of open field arena representing lower anxiety levels compared to WT (Fig 1A2, t=10.1, p<0.0001). Rearing, a risk assessment, investigating behavior[74], was found to be reduced in KOs (Fig 1A4, t=2.055, p=0.0431). Therefore, the behavioral assessment of *Tmod2* KOs in an open field suggests a novelty-induced locomotor activity with decreased anxiety levels and diminished risk assessment or an increased propensity for risk-taking behavior.

Low anxiety and risk taking behavior towards aversive context

Behavioral assessment was carried out in a standard light-dark box with 2 zones with different light intensity. A brightly lit area is aversive and mice prefer the dark side. Exploration of the light side, measured by the amount of time in the dark compared to the light side and the number of transitions between the two sides, is a form of risk-taking and anxiety behavior[75]. *Tmod2* KO spent significantly less time in dark compared to WT (Fig 1B1, t=3.72, p=0.0004) and had a greater number of transitions between light and dark zone (Fig 1B2, t=3.382, p=0.0011). This assay provides complementary evidence of the novelty-induced hyperactivity, increased risk-taking, and low anxiety behavior in *Tmod2* KO that was seen in the open field assay.

Intact general exploratory behavior, sensory motor gating, and motor coordination and learning

Even though *Tmod2* KO appears to be hyperactive and less anxious in a novel environment, other parameters such as general exploration, sensory-motor gating, and motor learning are intact. General exploration is measured using the hole-board apparatus that consists of a floor with multiple holes (16 in total) and elicits an exploratory head-dipping exploratory behavior. Total head dips in a 20 min window were found to be comparable in *Tmod2* KO and WT (Fig 1C, t=0.06607, p=0.9475), indicating no deficits in general exploration behavior in *Tmod2* KO.

Sensory-motor gating is measured using paired-pulse inhibition protocol. This behavioral assay was carried out in a sound-attenuated chamber. Startle response amplitude (Fig 1D1, t=0.4508, p=0.6534) and percent inhibition to an increasing levels of pre-pulse sound prior to aversive sound stimuli were found to

be comparable in KOs and WT (Fig 1D2, genotype, $F(1,240)=1.17$; $p=0.2805$; sound intensity, $F(2,240)=80.02$, $p<0.0001$; genotype X sound intensity, $F(2,240)=0.6452$, $p=0.5255$), indicating unperturbed sensory motor gating in *Tmod2* KO. Effects of *Tmod2* deletion on motor-learning and coordination is assessed using the rotarod test. In this test, motor-learning is tested by calculating mean latency to fall in 5 consecutive trials on accelerating cylindrical rod. *Tmod2* KO shows no deficits in motor coordination tasks and their performance was comparable to their WT counterparts (Fig 1E, $t=0.206$, $p=0.8373$).

Decreased body weight which is slightly biased towards loss of lean mass

KOMP phenotyping pipeline also involves weekly measurements of body weight between 5th-18th weeks of age. *Tmod2* KO males and females show a significant decline in body weight relative to WT that is more pronounced in late adulthood (10-12 weeks of age) (Fig 1F, genotype, $F(1,42)=11.59$, $p=0.001$; age X genotype, $F(13,546)=10.38$, $p<0.0001$; age X sex, $F(13,546)=19.67$, $p<0.0001$; genotype X sex, $F(1,42)=0.001$, $p=0.9741$). Further exploration of body composition data from microCT scans revealed an increased lean body mass (Supplementary Fig S1E, $t=2.437$, $p=0.017$), suggestive of decreased fat mass (Fig S1F, $t=1.719$, $p=0.0893$) and a significant reduction in body length (Fig S1D, $t=4.43$, $p<0.0001$) in *Tmod2* KO. Therefore, an age-dependent decrease in body weight in *Tmod2* KO is due to a modified lean vs fat mass ratio and hindered overall body growth or a combination of both. These data indicate that the *Tmod2* KO mice are approximately 22-28% smaller starting at 10-11 weeks of age. Although smaller, these mice had no overt phenotype(s) and did not show any signs of illness or poor health. Combined, KOMP data demonstrate specific behavior signatures in *Tmod2* KO that have been shown previously to be predictive of addiction, while several other parameters were found unchanged when compared to WT counterparts (see also Supplementary Fig S1).

Comprehensive phenotyping for addiction-relevant behavior

Based on KOMP results we generated a *Tmod2* KO colony and carried out addiction phenotyping. Prior to any behavioral analysis, we confirmed that TMOD2 was absent through western blot analysis. The

results confirmed the absence of TMOD2 protein in the mutant's cortical punches (Fig 2A). In addition, later genomics analysis showed reduced levels of *Tmod2* transcript (Fig 3D).

Unaffected acute response to low and high doses of cocaine

Separate groups of WT and KO mice were acutely injected with cocaine (10 or 20 mg/kg) and their locomotor response was analyzed 30 min before and 1h following injections. (Fig 2B-C). For statistical comparison, the net locomotor response was calculated by subtracting the total locomotor activity in a 30 min period following cocaine injections with the locomotor activity during 30 min baseline. Net locomotor response was found to be comparable between mutants and WT for both doses of cocaine indicating that the neural circuit that evokes acute drug-induced locomotor response is intact in *Tmod2* KO (Fig 2D, genotype, $F(1,89)=0.509$, $p=0.4789$; dose, $F(1,89)=10.07$, $p=0.0021$; genotype X dose, $F(1,89)=0.08954$, $p=0.7655$).

Cocaine-induced behavioral sensitization is impaired in Tmod2 KO

Repeated administration of psychostimulants such as cocaine evokes behavioral sensitization - a progressive and persistent amplification of locomotor response to the same dose of the drug. Sensitization is a hallmark of many drugs of abuse and is due to neuroadaptations in the reward circuit[76, 77]. Although it is only partially predictive of self-administration, a sensitization paradigm is often used to gauge plasticity in the mesolimbic circuit[78]. Our sensitization protocol consists of once-daily injections of saline for 4 consecutive days (test day 1-4), followed by 6, non-contingent, cocaine injections (15mg/kg, test day 5-10) and a saline injection on test day 11 (Fig 2E1). Since sensitization has been shown to be long-lasting[79], we carry out a cocaine challenge on test day 17 and 24, a period of 1 or 2 weeks later. Repeated administration of cocaine resulted in progressive amplification of locomotor responses in WT mice (Fig 2E1). Intriguingly, *Tmod2* KO had a significant attenuation of the cocaine-induced sensitization response compared to WT (Fig 2E1, genotype, $F(1,806)=252$, $p<0.0001$; drug, $F(12,806)=51.42$, $p<0.0001$; genotype X drug, $F(12,806)=11.34$, $p<0.0001$). *Tmod2* KOs show slight sensitized responses to the first three cocaine injections (day 5-7) with an increase in locomotor activity, but from the 4th day onwards

(day 8-10) and on cocaine challenge days (day 14 and 24), no further escalation in locomotor activity was observed (Fig 2E1). It is worth noting that a weak, drug-induced sensitization response is exhibited by *Tmod2* KO on day 5-7 with an early-achieved ceiling effect that stabilizes locomotor response from the 8th day onwards and persists for rest of the protocol. Post hoc analysis confirmed the absence of any locomotor differences between mutant and WT to acute cocaine administration (Fig 2E1, day 5, 1st cocaine administration, p=0.8109). These data indicate an impaired behavioral sensitization response in *Tmod2* KO suggestive of compromised drug-induced neuroadaptations.

Multiple exposures to a similar environmental context attenuates novelty-induced locomotor activity and leads to habituation: a form of non-associative learning[80]. In our analysis of sensitization data, we observed that *Tmod2* KO mice were not hyperactive in the open field upon repeated testing, indicating high rates of habituation. Pre-injection baseline periods (-60 to 0 min) of the first 4 saline days of behavioral sensitization paradigm were used to reconfirm the open-field phenotype observed in the KOMP analysis. *Tmod2* KO exhibited persistent, elevated locomotor activity, compared to WT on day 1 (Fig 2E2-Day 1, genotype, F(1,1100)=147.5, p<0.0001; time-bins, F(10,1100)=25.1, p<0.0001; genotype X time-bins, F(10,1100)=0.5143, p=0.8809). A main effect of genotype was also detected on day 2 (Fig 2E2-Day 2, genotype, F(1,1100)=4.995, p=0.0256; time-bins, F(10,1100)=6.166, p<0.0001; genotype X time-bins, F(10,1100)=1.007, p=0.4356) however, the post hoc analysis revealed that the time-bins significance was restricted to the first, 5-minute bin with WT having more locomotor activity compared to *Tmod2* KO (Fig 2E2-Day 2, Sidak's multiple comparison, p=0.0245). On day 3 (Fig 2E2-Day 3, genotype, F(1,1100)=2.298, p=0.1298; time-bins, F(10,1100)=18.07, p<0.0001; genotype X time-bins, F(10,1100)=0.9725, p=0.4656) and day 4 (Fig 2E2-Day 4, genotype, F(1,1100)=0.5777, p=0.4474; time-bins, F(10,1100)=14.34, p<0.0001; genotype X time-bins, F(10,1100)=1.211, p=0.2794), a main effect of genotype and post-hoc time-bins comparison failed to detect any statistically significant difference between *Tmod2* KO and WT. Similarly, on day 1, center distance traveled (Fig 2E3, D1, t=5.386, p<0.001) and time-spent in the center (Fig 2E4, D1, t=6.559, p<0.001) is significantly higher in *Tmod2*

KO recapitulating the results obtained from KOMP data. However, from the 2nd day onwards (D2-D4, Fig 2E3-4), these anxiety parameters are comparable in both the genotypes indicating an amplified habituation response to a less novel, familiar environmental context in *Tmod2* KO. This analysis demonstrates that the hyperactivity in *Tmod2* KO is a specific response towards environmental novelty that is only seen on the first day of the open field test and is not due to general hyperactivity. Thus, habituation, a form of non-associative learning is preserved and perhaps increased, in *Tmod2* KO. Combined, these data suggest that experience and pathway-specific neuroadaptations that mediate habituation are functional in *Tmod2* KO, while specific deficits are seen in neuroadaptations that mediate behavioral sensitization.

Failure to acquire cocaine self-administration

Although locomotor sensitization is an excellent model of drug-induced plasticity and neuroadaptations, it is only partially predictive of voluntary drug intake[78]. Goal-directed behavior and motivation to procure drug is conventionally tested by intravenous self-administration assay (IVSA), the gold standard technique in the addiction field[81]. Therefore, we assessed cocaine acquisition and dose-response in *Tmod2* KO and WT using the IVSA paradigm.

To assess cocaine IVSA performance, we performed repeated measures or one-way ANOVA using the number of lever presses or number of infusions as dependent measures. Genotype (*Tmod2* KO, WT) and sex were between-subject factors. Session (day 1 - 5) was a within-subjects factor. When lever presses were used as the dependent measure, lever (active, inactive) was used as a second within-subjects factor. WT mice rapidly learned to lever press for cocaine (Figure 2F) as indicated by a significant increase in active lever presses across sessions (day 1 vs day 5: $p = .05$) and a significant dissociation between the active and inactive levers (active vs inactive on s5: $p = .002$). In contrast, *Tmod2* KO mice failed to acquire cocaine infusions as indicated by a failure to significantly increase active lever presses across sessions (day 1 vs day 5: $p = 0.67$) and a failure to dissociate between the active and inactive lever (active vs inactive on day 5: $p = 0.82$). This lever pressing pattern resulted in WT mice infusing significantly

more cocaine across the first five sessions relative to *Tmod2* KO mice (Fig 2F inset, $p<0.05$). Lever pressing was mediated by strain and lever as indicated by significant main effects of strain [$F(1, 26) = 5.00$, $p = .03$] and lever [$F(1, 26) = 12.84$, $p = .001$], as well as a significant strain X lever interaction [$F(1, 26) = 4.64$, $p = .04$]. Interestingly, active lever press were comparable on day 1 indicating that general exploration and responses to operant cues are able to evoke behavior directed to the levers in *Tmod2* KO. However, either neutral or aversive outcome of active lever press rapidly extinguishes the future responses towards the active lever.

Comparison of WT and *Tmod2* KO mice on cocaine IVSA was limited to the acquisition phase because WT mice stabilized at the 1.0 mg/kg/infusion acquisition dose and advanced to the dose-response curve stage by session five. *Tmod2* KO mice were tested for a total of 24 sessions (Fig 2F) to test if they could learn to acquire cocaine if sufficient exposure was provided. During these 24 sessions, *Tmod2* KO mice failed to significantly increase response on the active lever and failed to dissociate between the active and inactive lever as indicated by nonsignificant main effects of lever ($p = 0.95$) and session ($p = 0.24$) as well as a nonsignificant lever x session interaction ($p = 0.33$). Since the mice failed to acquire, cocaine IVSA testing was terminated for *Tmod2* KO mice after session 24. IVSA results demonstrate that the dose which is reinforcing to WT mice is not reinforcing to KO mice and indicates either general reward deficits, learning deficits in an operant task, or both. Additionally, modified cocaine metabolism could also contribute to lack of acquisition and low locomotor sensitization in *Tmod2* KO.

Intact motivation towards natural reward

In order to investigate the responsivity to natural reward and to rule out a general deficit in reward-based learning, we subjected mice to a two-bottle sucrose preference test. Both strains show comparable motivation and preference towards 4% sucrose solution provided in the sucrose preference test (Fig 2G, $t=1.055$, $p=0.3108$). Therefore, inability of *Tmod2* KO to self-administer cocaine is not because of a general deficit in reward-sensing and responding neural circuitry.

Cocaine metabolism is unaffected in Tmod2 KO mice

In vivo cocaine metabolism is an important determinant of its pharmacokinetics and tissue bioavailability that could modulate a drug-induced addiction-like phenotype. To test cocaine metabolism in these mice we carried out a biochemical analysis for primary cocaine metabolite benzoylecgonine[82] by injecting mice with cocaine (20mg/kg) and collecting blood from the submandibular vein at 0, 10, 30, 60, and 120 min following injections. No significant differences in the level of the cocaine metabolite, benzoylecgonine, was observed between *Tmod2* KO and WT mice for any of the sampled time points, indicating that cocaine metabolism is not affected in these mutants (Fig 2H).

Delayed learning ability in operant assay

Since *Tmod2* has previously been shown to regulate learning and memory deficits in mice[17] and has been linked to intellectual deficits in human GWAS studies[44, 45], we tested whether the KO mice were capable of learning an operant task. Operant conditioning relies on associative learning abilities and therefore, the impairment to acquire cocaine in the IVSA paradigm could be due to learning deficits. We investigated operant learning in *Tmod2* KO mice for palatable food rewards as a reinforcement stimulus. *Tmod2* KO mice took significantly more number of trials to learn the association between active lever and palatable food reward, and to discriminate between the active and inactive lever (Fig 2I1). In contrast, WT mice learned to discriminate between the active and inactive lever by the end of day 1, demonstrating stronger associative learning than *Tmod2* KOs (Fig 2I1, genotype & lever, $F(3,242)=117.9$, $p<0.0001$; day, $F(9,242)=0.7612$, $p=0.6525$; genotype & lever X day, $F(27,242)=1.347$, $p=0.1244$). In *Tmod2* KO, statistically significant discrimination between the active and inactive lever emerges on day 8, and from day 7 onwards, active lever presses by KO and WT are comparable (Fig 2I1). Surprisingly, operant efficiency (number of sucrose pellets obtained divided by total number of active and inactive lever press) was found to be slightly better in *Tmod2* KO. We hypothesize that this is due to compulsive lever pressing by WT mice during initial trials (Fig 4F1, day 1-5) ignoring the 20 s timeout period between two successful (paired with reward) active lever presses (Fig 2I2, genotype, $F(1,115)=19.37$, $p<0.0001$; day,

F(9,115)=0.7663, p=0.6477; genotype X day, F(9,115)=1.554, p=0.1375). On extinction sessions (Fig 2I3, E1-E5 on day 11-15) during which neither reward nor operant cue (cue light off) were presented, both *Tmod2* KO and WT exhibited a comparable, rapid decline in the number of lever presses that was previously paired with reward indicating that extinction-induced associative learning is intact in both the genotypes (Fig 2I3, genotype F(1,66)=1.405, p=0.2401; day, F(5,66)=18.72, p<0.0001; genotype X day, F(5,66)=0.2839, p=0.9203). Rebound of behavior directed towards active lever with one single reinstatement session was also comparable between *Tmod2* KO and WT mice (Fig 2I3, R1, day 16, Sidak's post hoc test, p=0.79). Thus, as shown previously, *Tmod2* KO mice have a deficit in learning[17]. However given enough time, *Tmod2* KO mice can learn an operant task. In trials with food reward, *Tmod2* KO mice were indistinguishable from WT mice from day 7, whereas with cocaine as a reinforcement *Tmod2* KO failed to learn even after 24 day trial, which leads us to conclude that there is a deficit in cocaine-induced reward learning in *Tmod2* KO mice.

Reduced brain volume and absence of differentially coexpressed transcripts

Since neuron-specific TMOD2 regulates actin stabilization and plays an important role in dendritic arborization, and synapse formation[39, 40], we investigated if regional and gross morphological changes are seen in *Tmod2* KO brains. We carried out MR imaging, a well-established diagnostic and translational tool in clinical and preclinical research, and discovered that whole-brain volume is significantly decreased in *Tmod2* KO relative to the WT mice (Fig 3A-B, -8.8%, $p=1.5\times10^{-9}$). The extent of volume loss appears to be greater in white matter, as the overall changes for gray and white matter were -8.2% ($p=4\times10^{-9}$) and -14.7% ($p=7\times10^{-12}$) respectively (Fig 3A). The volumes of 182 structures (using combined left-right volumes) were computed for all animals. While the 20-25% decrease in body weight in 10-11 week-old *Tmod2* KO (Fig 1F) may explain some of this change, proportional weight change is not generally a predictor of proportional brain volume change in adult rodents[83, 84].

For the absolute volume analysis, a total of 109 structures were observed to be significantly different for the *Tmod2* KO mice (q<0.05), all but one of which were volume decreases. Prominent changes included

regions of the cerebellum, much of the cortex, the corpus callosum, the thalamus, the hippocampus, and, with relevance to the mesolimbic system, the striatum and midbrain (summarized in Supplemental Table S2). However, given the overall difference in brain size, we also normalized results by expressing structure volume as a percentage of whole-brain volume, and then comparing results. A total of 39 brain structures showed a significant difference in relative volume (Fig 3B). Several of the regions decreased in absolute size were still observed to be decreased in this analysis, especially the white matter regions (Fig 3B, 3C blue bars), but several structures also appeared relatively larger (Fig 3B, 3C red bars), including the hypothalamus, olfactory bulbs, nucleus accumbens and basal forebrain.

We next, attempted to detect any molecular differences that may have resulted from the deletion of *Tmod2* gene. Specifically, we hypothesized differences in cell type constituency, cell loss, neuroinflammation, neurodegeneration, or general developmental deficits that may be cell-type specific and thus, would lead to changes in gene co-expression networks that could be detected by monitoring of genome-wide gene expression[85, 86]. We carried out RNAseq analysis from striatum and cortex of naïve adult mice (3M/3F) for *Tmod2* KO and WT animals. A PolyA enriched RNA sequencing library was generated at a depth of 40-50 million reads. Data were analyzed using BioJupies[87]. As expected, we detected a clear difference in *Tmod2* RNA levels in both tissues (Fig 3D, FDR<0.05, q=0.005 and 0.002 in cortex and striatum, respectively). Unexpectedly, we observed very few other genes that were significantly misregulated (Supplemental Table S3). As a control analysis, we compared striatum and cortex gene expression in WT animals and found over 7439 genes (Supplemental Table S3) that were differentially expressed in these regions (Fig 3E, FDR<0.05). These genomics results indicate that there are no changes in gene coexpression networks that are detectable using bulk RNAseq analysis given our power. Thus, even though *Tmod2* KO have emotionality phenotypes associated with changes in brain volume, the transcriptomic analysis indicates a neural system that, for the most part, has a normal constituency. This led us to hypothesize that the observed behavioral changes are due to functional differences that may be detectable using electrophysiological methods.

Enhanced cortical excitability during development and adulthood

Since TMOD2 regulates dendritic arborization[39, 88], synapse density and maturation, and synaptic plasticity[39, 40, 89], we hypothesized that the firing properties of neurons might be modified due to altered synaptic connectivity. To test this, we harvested cortical cells from P0-P1 pups and quantified the spontaneous firing features of cultured neurons on MEA plates. We also tested the effect of GABA-A receptor and AMPA receptor antagonism on spontaneous activity (Fig 4B). MEA captures *in vitro* real-time electrophysiological activity and interconnectivity between cultured neurons permitting recreation of complex firing patterns and detection of deficits in a high-throughput fashion. *Tmod2* protein expression was detected in the rat brain as early as embryonic day 14 (E14) and attained adult-level expression by E19[42]. Embryo imaging data collected on *Tmod2* KO by KOMP phenotyping reveals robust, nervous system-specific LacZ expression driven by the *Tmod2* promoter at E12.5 (Fig 4A). This early developmental expression of *Tmod2* in mouse embryos suggests a critical function that could be compromised in *Tmod2* KO. *Tmod2* KO cortical neurons discharged at a higher frequency in a drug-free condition (Fig 4C-E1, t=3.547, p=0.0045). Picrotoxin, a potent GABA-A receptor blocker, failed to affect the firing rate in *Tmod2* KO cultures, whereas WT neurons respond with a three-fold change in firing rate (Fig 4E2, t=2.899, p=0.0327). This could be due to fewer functional, membrane-bound GABA-A receptors in *Tmod2* KO neurons or the absence of presynaptic GABAergic innervations or both. Absence or decrease in inhibitory tone to cultured neurons could also explain increased firing rate in *Tmod2* KO cortical cultures. Similarly, *Tmod2* KO neurons produce significantly more bursts in the drug-free baseline condition (Fig 4F1, t=4.392, p=0.0011). Picrotoxin application resulted in an eight-fold increase in burst number in WT neurons and has no effect on *Tmod2* KO neurons suggesting altered GABA receptor availability or GABAergic synapses or both (Fig 4F2, t=4.538, 0.0094). NBQX application prevents bursting in WT cortical neurons while the *Tmod2* KO neurons showed a similar tendency, but did not reach our statistical cutoff (Fig 4F2, t=2.391, p=0.0863). Synchronicity among cultured neurons to fire simultaneously is significantly elevated in *Tmod2* KO neurons (Fig 4G1, t=5.133, p=0.0003). PTX

application resulted in a four-fold increase in firing synchronization of WT cortical neurons and had no effect on *Tmod2* KO neurons (Fig 4G2, t=4.947, p=0.003). As anticipated, NBQX application mitigates the synchrony index in WT neurons but not in *Tmod2* KO (Fig 4G2, t=3.16, p=0.0134). These results clearly demonstrate that *Tmod2* KO neurons in culture exhibit enhanced cortical excitability along with modified excitation/inhibition ratio during early developmental stages.

To test whether neuronal excitability persists in adult *Tmod2* KO mice, we compared intrinsic properties of prelimbic cortical (Fig 4H1-5) and accumbens shell neurons (Fig 4I1-5) in KO and WT using whole-cell recording in acute brain slices. Naïve mice were sacrificed and brain slices containing prelimbic and accumbens region neurons were recorded. *Tmod2* KO cortical neurons fired more action potential spikes in response to depolarizing current steps than WT neurons (Fig 4H1-2). *Tmod2* KO neurons showed slightly higher resting membrane potentials than WT neurons (Fig 4H3), but no change in input resistance or whole cell capacitance (Fig. 4H4-H5). The action potential threshold (data not shown; -39.51 ± 0.46 mV in WT and -38.6 ± 0.53 in *Tmod2* KO) and after-hyperpolarization amplitude (data not shown; 12.11 ± 0.62 mV in WT and 13.48 ± 0.76 mV in *Tmod2* KO) are statistically comparable between genotypes indicating functional similarity of voltage-gated sodium channels and potassium channels. *Tmod2* KO accumbens shell neurons are also more excitable than WT (Fig 4I1-2), but no change in resting membrane potential was observed (Fig 4I3). The input resistance is slightly higher in *Tmod2* KO neurons (Fig 4I4), and whole cell capacitance is comparable between both genotypes (Fig 4I5). The action potential threshold (data not shown; -35.69 ± 0.98 mV in WT, -35.67 ± 0.59 mV in *Tmod2* KO) and after-hyperpolarization amplitude (data not shown; 12.05 ± 1.03 mV in WT and 12.07 ± 0.52 mV in *Tmod2* KO) are statistically comparable between genotypes. Therefore, *Tmod2* deletion results in an increase in excitability of prelimbic pyramidal neurons, and medium spiny neurons of accumbens shell, indicative of its role in determining the firing features of neurons and their interconnectivity.

Distinct naïve and cocaine-induced synaptic properties

Action-potential independent, spontaneous release of neurotransmitters from presynaptic neurons and measurement of the miniature excitatory or inhibitory postsynaptic currents is a standard method to assess the baseline and drug-induced alteration in synaptic coupling between neurons. Non-contingent cocaine administration induces widespread modifications of synaptic properties in reward-related brain regions, triggering maladaptive reward learning[1]. These synaptic alterations have been extensively characterized in nucleus accumbens and establish both effect and causality of cocaine abuse[90]. *Tmod2* KO mice have an attenuated locomotor sensitization response to repeated cocaine administration and perform poorly in an IVSA paradigm. We hypothesized that drug-induced synaptic changes are either missing or weak in *Tmod2* KO resulting in a drug-resistant phenotype. Mice were either treated with a once-daily injection of saline or cocaine for 5 consecutive days, sacrificed following 2-5 day of abstinence and brain slices containing accumbens region neurons were recorded (Fig 5B). We compared mEPSC (Fig 5C1) and mIPSC (Fig 5D1) in medium spiny projection neurons of accumbens shell (Fig 5A) in drug-naïve (saline injected) and drug-experienced (cocaine injected) mice using *ex vivo* whole-cell recording in brain slices. Mean amplitude of mEPSCs is significantly elevated in naïve *Tmod2* KO compared with naïve WT neurons (Fig 5C2), which suggests an increased number or function of AMPA receptors on patched accumbens neurons[91]. Cocaine treatment increases mEPSC frequency in WT but not *Tmod2* KO neurons (Fig 5B3), suggesting that repeated cocaine exposure fails to induce synaptic changes typically associated with chronic cocaine exposure[92]. No significant effect of treatment or genotype was observed in either mEPSC rise or decay time which indicates a lack of alterations in the postsynaptic properties of AMPA receptors (Fig 5C4-C5).

Medium spiny neurons of accumbens shell receive inhibitory afferents from local interneurons, cortex and VTA[93, 94]. There is no change in mIPSC amplitude in WT and KO with or without drug exposure (Fig 5D2). However, mIPSC frequency is higher in naïve KO neurons than naïve WT neurons, and cocaine exposure increases mIPSC frequency in KO but not WT neurons (Fig 5D3). Elevated mIPSC frequency

in *Tmod2* KO could be a neurophysiological homeostatic adaptation to compensate for increased excitability of accumbens shell neurons due to modified intrinsic and excitatory synaptic properties[95]. Rise and decay time of mIPSCs are not different in WT and KO and unaffected by cocaine exposure (Fig 5D4-D5). Combined, investigation of synaptic properties indicates preexisting and drug-induced differences in excitatory pre- and post-synaptic neurotransmission, along with augmented presynaptic inhibitory neurotransmission. These data provide a mechanistic underpinning for the lack of sensitization and acquisition in the IVSA paradigm.

Discussion

Our work describes a critical role for *Tmod2* in drug-induced behavioral sensitization and voluntary drug intake. *Tmod2* has been weakly linked to risky drug use in humans and its gene expression and protein levels are dynamic upon drug exposure in animal models[46-53]. We provide behavioral data that *Tmod2* regulates sensitization and IVSA of cocaine in mice. Furthermore, despite changes in brain volume, transcriptomics analysis found no detectable changes in gene co-expression signatures in *Tmod2* KO. Concordant with this, we find that the acute locomotor response to cocaine is not affected in *Tmod2* KO. *Tmod2* mediates dendritic branching, spine maturation and density, and synaptic plasticity; the key components of experience-induced learning and memory including addiction[17, 39, 40, 96]. Thus, we reasoned that drug-induced plasticity may be affected in these knockouts. We found a lack of sensitization upon repeated administration of the cocaine. Deletion of *Tmod2* leads to an imbalance of excitatory and inhibitory signaling as well as compromised synaptic plasticity in the mesolimbic reward circuit, which we propose as a causal mechanism for the cocaine relevant behavioral differences. Thus, behavioral and electrophysiological data indicate neuromodulations that mediate transition to addiction are compromised in the absence of *Tmod2*.

We characterized these mutants for various cocaine-induced behaviors such as acute response to cocaine, locomotor sensitization following non-contingent repeated cocaine administration and cocaine self-administration, to conclude that *Tmod2* KO have reduced cocaine-induced locomotor sensitization and are resilient to the reinforcing effects of cocaine. Structural and functional plasticity of synapses are the fundamental mechanisms that underlie addiction even though the role of actin in this process remains controversial [2, 11, 30, 97]. Acute or chronic cocaine exposure, as well as abstinence, facilitates dendritic spine outgrowth and spine density in reward-related brain regions such as prefrontal cortex and nucleus accumbens[31, 32, 92, 98, 99]. Our previous study established a role of *Cyfip2*, a component of the WAVE regulatory complex that mediates branched actin formation. We demonstrated that a *Cyfip2* mutation that exists in certain C57BL/6 substrains leads to altered acute and sensitized responses to cocaine[21].

Despite a role in the structural and synaptic plasticity that is the cellular basis of learning and addiction-related maladaptive behavior, the role of actin-regulating *Tmod2* in addiction has previously been unclear. Here we report that *Tmod2* KO mice exhibit endophenotypes that are predictive of addiction, but surprisingly exhibit resistance to drug-induced behaviors and associated neuroadaptations. Typically, hyperactivity, novelty-reactivity, anxiety, and risk-taking behavior in *Tmod2* KO are associated with increased risk of addiction[72, 100-102]. However, the lack of TMOD2 seems to be protective, perhaps due to modifications in intrinsic and synaptic properties of reward regions that regulate reward learning[90, 103]. In support of this idea preexisting hyperexcitability of prefrontal and ventral striatum neurons in *Tmod2* mutants could actively resist the cocaine-induced depression of these regions, thereby masking the maladaptive behavioral effects of cocaine[104, 105]. Interestingly, high frequency (5-20 hz) transcranial magnetic stimulation that increases cortical excitability has been shown to be an effective treatment for cocaine craving[106-108], indicating that cortical excitability in naive *Tmod2* KO could interfere and prevent cocaine-induced addiction behavior. Basal and cocaine-induced changes in synaptic properties of accumbens neurons are also distinct from their WT counterparts and support behavioral results. Specifically, a preexisting amplified amplitude of excitatory glutamatergic synapses and unaffected release probability from presynaptic neurons on *Tmod2* KO striatal neurons demonstrate altered AMPA receptor number or function, and absence of cocaine-induced presynaptic plasticity[109, 110]. Similarly, accumbens shell neurons exhibit modified, drug-independent inhibitory presynaptic responses that is further aggravated by chronic drug exposure. Although drug-induced excitatory synaptic events are well characterized in nucleus accumbens, little is known about inhibitory synapses and how they responds to repeated cocaine challenge. Previous reports suggest an absence and decrease in the postsynaptic and presynaptic strengthening of inhibitory neurotransmission following cocaine exposure, respectively[110]. Intriguingly, although available literature is heavily biased towards the role of TMOD2 in the postsynaptic dendritic compartment, our study clearly shows presynaptic effects on neurotransmission leading to frequency modulation in excitatory and inhibitory synapses. Interestingly, the acute locomotor

response to cocaine is not affected in *Tmod2* KO demonstrating that the basal ganglia circuit, which regulates drug-induced locomotor activation, is not perturbed[111].

Drug-independent functional plasticity differences observed in cortical and striatal regions in our study, and in the hippocampus by other labs, seems to reveal a potential mechanism for the learning phenotype exhibited by these mutants[17, 96]. Operant learning is a form of associative learning that is dependent on various brain regions including nucleus accumbens and hippocampus[112, 113]. *Tmod2* KO show deficits in associative learning with delayed performance in operant conditioning, but has no deficits in motor learning as determined by the rotarod assay. In addition, KO mice show enhanced non-associative learning which is demonstrated by enhanced habituation of hyperactivity and anxiety measures in the open field. Recent human GWAS and meta-analysis study revealed an intronic variant of *Tmod2* to be correlated with intellectual disability[44] and intelligence in general[45]; suggestive of an important role for this gene in influencing normal cognitive functions in human and animal models. Rotarod data from KOMP indicates that Tmod2 deletion does not affect motor learning and our habituation analysis of open field data shows intra- and inter-session habituation, a form of non-associative learning that is normal or perhaps enhanced in the knockouts. Thus, in the KO mice there are specific learning deficits that are regulated by *Tmod2*. Our electrophysiology results will be of interest to learning and cognition researchers interested in the function of *Tmod2*.

Since *Tmod2* is an actin-regulator[88], mutants were tested for structural anomalies of the brain using MRI. We found a ~9% reduction of total brain volume, with 60% of the structures evaluated across the brain affected. However, after correction for differences in whole brain size (accounting for global volume differences), a smaller number of key structural differences were isolated: (1) decreased volumes across a number of regions notably including white matter structures and the thalamus; and (2) volume increases over a number of regions including the basal forebrain and the nucleus accumbens. Comparable human MRI studies of addiction include reports of a number of morphological or microstructural changes related to the regions identified in the *Tmod2* KO mice. For example, decreased fractional anisotropy, indicating

abnormality in the white matter, has been reported in the frontal white matter[114] and in the corpus callosum[115] of cocaine-dependent individuals. The thalamus, frequently linked to addiction, has also been studied frequently, but morphological findings are inconsistent, with volume increases, decreases or no change reported[116]. More consistent findings have been observed in the nucleus accumbens, where decreased volumes have been identified in crack-cocaine users[116] and increased volumes are associated with the duration of abstinence (from alcohol, cannabis, and/or cocaine) in former users[117]. It remains unclear in these human studies, however, whether the morphological findings predate or emerge after substance use. Given that the *Tmod2* KO mice evaluated by MRI in this study were cocaine naïve, it is difficult to relate the morphological findings directly to human observations. Although we did not perform measurements of fractional anisotropy in this work, the smaller white matter volumes in the *Tmod2* KO mice may be inconsistent with changes observed in humans, in which microstructural changes evident in fractional anisotropy were linked with drug use. In *in vitro* cell cultures, TMOD2 has been shown to negatively regulate neurite formation[118] and, therefore, *Tmod2* deletion might be expected to lead to increased white matter volume in our study. This discrepancy could arise due to limited physiological relevance of *in vitro* cell cultures that fails to mimic the complex developmental processes required for axonal pathfinding and white matter development. It seems unlikely that the decreased white matter volume in the *Tmod2* KO mice is linked with the addiction phenotype. On the other hand, the larger relative volume of the nucleus accumbens in *Tmod2* KO mice, and the corresponding reduced IVSA, appears consistent with the expectations from human findings that an increased accumbens volume would be associated with a reduced addiction phenotype. Of course, the morphological changes observed in the *Tmod2* KO mice represent the net result of a complex developmental process, including influences of altered synapse formation and/or function. Thus, like the behavioral phenotype, morphological changes may be secondary to other dysfunctional cellular processes. The complex interplay of these interactions is an ongoing topic in neurodevelopmental research.

RNAseq analysis performed in adult, naive mice show an absence of differentially expressed transcripts in cortex and striatum. Therefore, the transcriptional modifications could not be attributed to the phenotype observed in *Tmod2* KO. However, the negligible transcriptional modification induced by *Tmod2* deletion makes it a potential translational target that might be used to transiently modulate cocaine-induced actin dynamics and plasticity. Recently, non-muscle myosin IIB that regulates synaptic actin polymerization has been proposed as a potential therapeutic target for treatment of methamphetamine addiction, but was found to be ineffective against cocaine or morphine associated contextual memory[33, 119, 120]. Based on our results, *Tmod2* could be specifically pursued to target cocaine-induced neuroadaptation that results in a maladaptive phenotype. However, due to redundancy in the reward circuit, we speculate that the effect of *Tmod2* deletion could affect responses for a wide category of drugs.

Actin-regulating proteins with structural and functional neural remodeling properties are emerging as critical regulators of addiction. This study establishes a causal role for *Tmod2* in regulating addiction-predictive and addiction behavior in mice. The severe impairment in cocaine-based reward learning but no deficits in motor learning or non-associative learning, indicates specificity of TMOD2 function. Future studies with cell type and temporally specific *Tmod2* knockouts are required to tease apart this specificity and to address the developmental role of TMOD2 in the reward circuit. The neuronal restriction of *Tmod2* expression combined with its functional role in regulating cocaine intake could potentially be harnessed as a pharmacotherapy for addiction. The current findings combined with our previous results[21] emphasize the advantage of unbiased forward genetic approaches to studying addiction.

Author contributions

Conceptualization, VK and AM; Investigation, AM, SD, PED, JZ, JG, BJN, N-PT and VK; Writing, AM and VK; Editing and review, PED, JZ, BJN, RMH, N-PT, EJC and Z-WZ; Graphs and figure layout, AM, VK, JZ, N-PT and BJN; Funding acquisition, VK; Supervision, VK and Z-WZ.

Acknowledgements

We thank the members of the Kumar laboratory for their valuable input to this work especially Brain Geuther and Kevin Seburn for proofreading the manuscript and suggesting the layout of the figures. We also thank members of Dr. Zhong-Wei lab especially Dr. Guoqiang Hou for helping AM in setting up the electrophysiology rig for slice recordings. We thank Delia Hartley for her help with animal husbandry. We thank the entire KOMP team at The Jackson Laboratory – Jacqui White, Steve A. Murray, Robert E. Braun, James Clark, Pamelia Fraungruber, Rose Presby, Zachery Seavey, and Catherine Witmeyer. We also thank Heidi Munger and Jeremy Charette of Genome Technologies division at the Jackson Laboratory for their help in generating the RNA sequencing data. This work was supported by the NIDA grant the NIH National Institute on Drug Abuse 5P50DA039841 to E.J.C., U01DA041668 and Brain and Behavioral Foundation Young Investigator Award to V.K.

Figure legends

Figure 1. Behavioral characterization of *Tmod2* KO using publicly available data in KOMP repository shows specific deficits in hyperactivity and anxiety phenotypes.

(A1-A5) Open-field assay results; (A1) Distance travelled by wild type (WT) and tropomodulin-2 knockout (KO) in a 20 min exposure to standard open-field arena in four, 5 min bins show persistent locomotor hyperactivity. (*Bonferroni's multiple comparison post hoc test detected significant differences ($p<0.0001$) between WT and KO mice.) (A2) percentage of distance travelled in center and (A2) mean total time spent in center are significantly higher in KO. (A4) Number of rear postures performed by KO is significantly less than WT. (A5) Total time spent mobile is significantly more in KO. (B1-B2) LD box results; (B1) time spent in dark side of the LD box is significantly lower in KO. (B2) Number of transitions between light and dark regions of the LD box is significantly more in KO. (C) 20 min exposure to hole-board assay evokes comparable number of head dips from WT and KO mice. (D1-D2) Prepulse inhibition assay results; (D1) startle amplitude and (D2) percentage inhibition of reaction to a subsequent stronger acoustic stimulus is comparable in WT and KO. (E) Rotarod performance test shows no deficit of motor coordination in WT and KO. (F) Only those mouse that has body weight data for all the 14 weeks were taken for analysis (WT, n=30, 15 males, 15 females; KO, n=16, 8 males, 8 females). Body weight growth curve demonstrates significant effect of genotype and sex (*significantly different from same-sex *Tmod2* KO, $p<0.05$). Error bar represents SEM. OFA, open field assay; LD, light-dark box; HB, hole-board assay; PPi, paired-pulse inhibition; RR, rota-rod test; BW, body weight growth curve.

Figure 2. Comprehensive addiction phenotyping in *Tmod2* KO reveals deficits in cocaine sensitization and IVSA. (A) Qualitative assessment of absence of TMOD2 protein in cortical lysate from KO brain. (B) Locomotor response following acute injections of low (10 mg/kg i.p.) and (C) high (20 mg/kg i.p.) doses of cocaine are comparable in WT and KO mice. Green arrow head indicates locomotor artifact due to injection procedure. (D) Net locomotor activity following low and high dose of cocaine show no differences between WT and KO responses. (E1-E4) Results obtained from locomotor sensitization protocol. (E1) Graph's x-axis show day and corresponding treatment (S, saline; C, cocaine) on that day. Acute response (day 5) to cocaine detected no difference in WT and KO response. Second injection onwards (day 6-10, 17 and 24) KO mice exhibits attenuated locomotor sensitization to repeated cocaine injections whereas a progressive amplification of locomotor response is witnessed in WT. (E2) Day 1 baseline locomotor activity is significantly higher in KO. On day 3-4 there is no significant difference observed in WT and KO. (E3) Mean center distance travelled and (E4) time spent in center during baseline period on day 1, is significantly high in KO. (F) In cocaine IVSA, WT rapidly escalate active lever presses and acquires the self-administration threshold in 5 days, while KO failed to discriminate between active and inactive lever and failed to acquire after 24 daily testing sessions. Inset show less number of cocaine infusions obtained by KO in first 5. (G) WT and KO equally prefers sucrose solution (4%) over water. (H) Cocaine metabolite benzoylecgonine concentration in plasma at different time points following cocaine (20 mg/kg) injections are comparable in WT and KO. (I1-I3) Operant conditioning using palatable food as a reinforcement resulted in (I1) rapid escalation of active lever press (day 1-5) in WT. KO mice required multiple sessions to learn the active lever-sucrose pellet reward association and gradually escalated active lever press that becomes comparable to WT by day 7. WT learns to discriminate between active and inactive lever from day 1, whereas in KO this discrimination emerges on day 8. (I2) Total sucrose pellets obtained by total number of active and inactive lever presses is calculated as percent efficiency and found to be significantly higher in KO. (I3) Extinction sessions (E1-E5 on day 11-15) and reinstatement (R1 on day 16) of reward behavior failed to detect any differences between WT and KO. Error bar represents SEM. ns, not significant. *Bonferroni's multiple

comparison post hoc test detected significant differences ($p<0.01$) between WT and KO mice. ***main effect of genotype detected using 2way ANOVA ($F_{10, 1100} = 25.10$, $p<0.0001$). #Significant difference between inactive and active lever press within same genotype ($p<0.01$).

Figure 3. MRI and bulk RNAseq analysis on WT and KO brains. (A) KO brain is about 8.8% smaller than WT reference mice. The extent of volume loss appears to be greater in white matter than gray matter. (B) KO strain differences based on relative volumes. Color overlays indicate volume changes referenced to the WT. (C) Relative volume differences of KO brain regions. Blue and red boxes indicate relative decrease and increase in volume of labelled brain region. Most of the blue boxes are associated with white matter regions in the brain. (D) Analysis of differentially expressed transcript in cortex and striatum found numerous hits indicating strong region-specific transcription profile. (E) Schematic of cortical punches obtained from M1 sub-region and dorso-ventral striatum (grey highlighted region) along with volcano plots of cortical and striatal differentially expressed genes in KO relative to WT. Except *Tmod2* in both brain regions and few other pseudogenes transcripts in striatum, no other transcript overcome the assigned threshold of FDR < 0.05. Error bar represents SEM. Blue circle indicate transcript that fulfills threshold criteria.

Figure 4. Characterization of spontaneous firing features of early postnatal cortical neurons and intrinsic properties of reward regions in adult brain. (A) Nervous system specific lacZ expression in KO embryo (E12.5) driven by *Tmod2* promotor and absence of expression in WT. (B) Timeline of multielectrode array (MEA) recordings of cultured cortical neurons. (C) Raw traces of spiking activity and offline spike sorting captured by MEA electrodes following PTX application in WT and KO cortical cultures. (D) Representative raster plots of spontaneous spiking activity in WT and KO neurons across 64 electrodes. (E1) Baseline spiking activity obtained from pre-drug window is significantly higher in KO neurons. (E2) PTX bath application resulted in increased firing rate in WT but not in KO. NBQX application has no effects on KO neurons while WT neurons respond with decrease in firing rate. (F1) Number of burst detected in 10 min pre-drug period is significantly higher in KO and (F2) unaffected by PTX and NBQX application. (G1) Synchrony index was found to be elevated in KO neurons. (G2) Both PTX and NBQX failed to modify responses of KO neurons (1 fold change). PTX increased, whereas NBQX decreased synchrony index of WT cortical neurons. (H1-H5) Intrinsic properties of adult, prelimbic pyramidal neurons. N= 23-38 neurons per genotype; 3-4 mice per genotype (H1) Schematic of whole-cell recordings performed in 5th layer of prelimbic cortex along with representative action potentials recorded by applying 160 pA for 700 ms. (H2) Mean number of spikes for a given magnitude of injected current is increased in KO cortical neurons. (H3) resting membrane potential is significantly elevated in KO. (H4) Input resistance of cortical neurons are comparable between WT and KO. (H5) Whole cell capacitance was found to be lower in KO. (I1-I5) Intrinsic properties of adult, accumbens shell medium spiny neurons (N = 9-28 neurons per genotype; 3-4 mice per genotype). (I1) Schematic of recorded brain region and samples traces at 200 pA. (I2) Mean number of spikes for a given magnitude of injected current is significantly increased in KO neurons. (I3) Resting membrane potential is comparable between genotypes. (I4) Input resistance is significantly increased in KO. (I5) Whole cell capacitance is not affected in KO. Error bar represents SEM. *$p<0.05$, **$p<0.01$, ***$p<0.001$. E12.5, embryonic day 12.5. PTX, GABA-A receptor blocker. NBQX, AMPA receptor antagonist. Prl, prelimbic. NAc, nucleus accumbens.

Figure 5. Electrophysiological characterization of glutamatergic and GABAergic synaptic transmission in accumbens shell medium spiny neurons. (A) Schematic of sagittal section of mouse brain containing recorded nucleus accumbens shell subregion. (B) Timeline of sensitization protocol in two groups. Saline (S, green) group mice were injected with non-contingent saline injections. Cocaine (C, purple) group

mice were injected with non-contingent cocaine (15 mg/kg, i.p.). Following 2-6 days of abstinence, mice were sacrificed and synaptic properties were recorded in ex vivo brain slices. (C1) representative traces showing mEPSCs at holding potential of -65 mV in the presence of 0.5 μM TTX in saline (top) or cocaine (bottom) injected WT and KO mice. (C2) mEPSC amplitude is not affected by cocaine exposure in both WT and KO. Saline treated KO mice has significantly elevated mEPSC amplitude. (C3) Cocaine exposure significantly increases mEPSC frequency in WT but not in KO. (C4-C5) mEPSC rise and decay time are not significantly different in WT and KO. Saline group: N = 13-16 neurons per genotype, 3-4 animals per genotype; cocaine group: (N = 22-27 neurons per genotype, 4-5 animals per genotype). (D1) representative traces showing mIPSCs at holding potential of +5 mV in presence of 0.5 μM TTX in saline (top) or cocaine (bottom) injected WT and KO mice. (D2) mIPSC amplitude is unaffected by treatment and between genotypes. (D3) Cocaine exposure increases mIPSC frequency in KO but not in WT. In saline injected mice, mIPSC frequency is significantly higher in KO. (D4-D5) mIPSC rise time and decay time show no significant effect of treatment or genotype. Saline group: N = 18-27 neurons per genotype, 3-4 animals per genotype; cocaine group: N = 25-31 neurons per genotype, 4-5 animals per genotype. Error bar represents SEM. *$p<0.01$.

References

1. Grueter BA, Rothwell PE, Malenka RC. Integrating synaptic plasticity and striatal circuit function in addiction. *Current opinion in neurobiology* 2012; **22**(3)**:** 545-551.

2. Rothenfluh A, Cowan CW. Emerging roles of actin cytoskeleton regulating enzymes in drug addiction: actin or reactin'? *Current opinion in neurobiology* 2013; **23**(4)**:** 507-512.

3. Volkow Nora D, Morales M. The Brain on Drugs: From Reward to Addiction. *Cell* 2015; **162**(4)**:** 712-725.

4. Miller EC, Zhang L, Dummer BW, Cariveau DR, Loh H, Law P-Y *et al.* Differential modulation of drug-induced structural and functional plasticity of dendritic spines. *Molecular pharmacology* 2012; **82**(2)**:** 333-343.

5. Kourrich S, Klug JR, Mayford M, Thomas MJ. AMPAR-independent effect of striatal αCaMKII promotes the sensitization of cocaine reward. *The Journal of neuroscience : the official journal of the Society for Neuroscience* 2012; **32**(19)**:** 6578-6586.

6. Thomas MJ, Beurrier C, Bonci A, Malenka RC. Long-term depression in the nucleus accumbens: a neural correlate of behavioral sensitization to cocaine. *Nature neuroscience* 2001; **4**(12)**:** 1217-1223.

7. Dong Y, Green T, Saal D, Marie H, Neve R, Nestler EJ *et al.* CREB modulates excitability of nucleus accumbens neurons. *Nature neuroscience* 2006; **9**(4)**:** 475-477.

8. Mu P, Moyer JT, Ishikawa M, Zhang Y, Panksepp J, Sorg BA *et al.* Exposure to cocaine dynamically regulates the intrinsic membrane excitability of nucleus accumbens neurons. *The Journal of neuroscience : the official journal of the Society for Neuroscience* 2010; **30**(10)**:** 3689-3699.

9. Peoples LL, Kravitz AV, Guillem K. The role of accumbal hypoactivity in cocaine addiction. *TheScientificWorldJournal* 2007; **7:** 22-45.

10. Yu J, Yan Y, Li K-L, Wang Y, Huang YH, Urban NN *et al.* Nucleus accumbens feedforward inhibition circuit promotes cocaine self-administration. *Proceedings of the National Academy of Sciences* 2017; **114**(41)**:** E8750.

11. Russo SJ, Dietz DM, Dumitriu D, Morrison JH, Malenka RC, Nestler EJ. The addicted synapse: mechanisms of synaptic and structural plasticity in nucleus accumbens. *Trends in neurosciences* 2010; **33**(6)**:** 267-276.

12. Deller T, Korte M, Chabanis S, Drakew A, Schwegler H, Stefani GG *et al.* Synaptopodin-deficient mice lack a spine apparatus and show deficits in synaptic plasticity. *Proc Natl Acad Sci U S A* 2003; **100**(18)**:** 10494-10499.

13. Feng J, Yan Z, Ferreira A, Tomizawa K, Liauw JA, Zhuo M *et al.* Spinophilin regulates the formation and function of dendritic spines. *Proc Natl Acad Sci U S A* 2000; **97**(16)**:** 9287-9292.

14. Kim MH, Choi J, Yang J, Chung W, Kim JH, Paik SK *et al.* Enhanced NMDA receptor-mediated synaptic transmission, enhanced long-term potentiation, and impaired learning and memory in mice lacking IRSp53. *The Journal of neuroscience : the official journal of the Society for Neuroscience* 2009; **29**(5)**:** 1586-1595.

15. Lin WH, Nebhan CA, Anderson BR, Webb DJ. Vasodilator-stimulated phosphoprotein (VASP) induces actin assembly in dendritic spines to promote their development and potentiate synaptic strength. *The Journal of biological chemistry* 2010; **285**(46)**:** 36010-36020.

16. Wu LJ, Ren M, Wang H, Kim SS, Cao X, Zhuo M. Neurabin contributes to hippocampal long-term potentiation and contextual fear memory. *PloS one* 2008; **3**(1)**:** e1407.

17. Cox PR, Fowler V, Xu B, Sweatt JD, Paylor R, Zoghbi HY. Mice lacking tropomodulin-2 show enhanced long-term potentiation, hyperactivity, and deficits in learning and memory. *Molecular and Cellular Neuroscience* 2003; **23**(1)**:** 1-12.

18. Offenhauser N, Castelletti D, Mapelli L, Soppo BE, Regondi MC, Rossi P *et al.* Increased ethanol resistance and consumption in Eps8 knockout mice correlates with altered actin dynamics. *Cell* 2006; **127**(1)**:** 213-226.

19. Furukawa K, Fu W, Li Y, Witke W, Kwiatkowski DJ, Mattson MP. The actin-severing protein gelsolin modulates calcium channel and NMDA receptor activities and vulnerability to excitotoxicity in hippocampal neurons. *The Journal of neuroscience : the official journal of the Society for Neuroscience* 1997; **17**(21)**:** 8178-8186.

20. Star EN, Kwiatkowski DJ, Murthy VN. Rapid turnover of actin in dendritic spines and its regulation by activity. *Nature neuroscience* 2002; **5**(3)**:** 239-246.

21. Kumar V, Kim K, Joseph C, Kourrich S, Yoo S-H, Huang HC *et al.* C57BL/6N mutation in cytoplasmic FMRP interacting protein 2 regulates cocaine response. *Science (New York, NY)* 2013; **342**(6165)**:** 1508-1512.

22. Soderling SH, Guire ES, Kaech S, White J, Zhang F, Schutz K *et al.* A WAVE-1 and WRP signaling complex regulates spine density, synaptic plasticity, and memory. *The Journal of neuroscience : the official journal of the Society for Neuroscience* 2007; **27**(2)**:** 355-365.

23. Pilo Boyl P, Di Nardo A, Mulle C, Sassoe-Pognetto M, Panzanelli P, Mele A *et al.* Profilin2 contributes to synaptic vesicle exocytosis, neuronal excitability, and novelty-seeking behavior. *The EMBO journal* 2007; **26**(12)**:** 2991-3002.

24. Li G, Wang Y, Yan M, Xu Y, Song X, Li Q *et al.* Inhibition of actin polymerization in the NAc shell inhibits morphine-induced CPP by disrupting its reconsolidation. *Sci Rep* 2015; **5:** 16283.

25. Toda S, Shen HW, Peters J, Cagle S, Kalivas PW. Cocaine increases actin cycling: effects in the reinstatement model of drug seeking. *The Journal of neuroscience : the official journal of the Society for Neuroscience* 2006; **26**(5)**:** 1579-1587.

26. Young EJ, Briggs SB, Miller CA. The Actin Cytoskeleton as a Therapeutic Target for the Prevention of Relapse to Methamphetamine Use. *CNS & neurological disorders drug targets* 2015; **14**(6)**:** 731-737.

27. Ojelade SA, Jia T, Rodan AR, Chenyang T, Kadrmas JL, Cattrell A *et al.* Rsu1 regulates ethanol consumption in Drosophila and humans. *Proceedings of the National Academy of Sciences* 2015; **112**(30)**:** E4085.

28. Gu Z, Fonseca V, Hai C-M. Nicotinic acetylcholine receptor mediates nicotine-induced actin cytoskeletal remodeling and extracellular matrix degradation by vascular smooth muscle cells. *Vascular pharmacology* 2013; **58**(1-2)**:** 87-97.

29. Ryder MI. Nicotine effects on neutrophil F-actin formation and calcium release: implications for tobacco use and pulmonary diseases. *Experimental lung research* 1994; **20**(4)**:** 283-296.

30. Miller EC, Zhang L, Dummer BW, Cariveau DR, Loh H, Law PY *et al.* Differential modulation of drug-induced structural and functional plasticity of dendritic spines. *Molecular pharmacology* 2012; **82**(2)**:** 333-343.

31. Norrholm SD, Bibb JA, Nestler EJ, Ouimet CC, Taylor JR, Greengard P. Cocaine-induced proliferation of dendritic spines in nucleus accumbens is dependent on the activity of cyclin-dependent kinase-5. *Neuroscience* 2003; **116**(1)**:** 19-22.

32. Robinson TE, Kolb B. Alterations in the morphology of dendrites and dendritic spines in the nucleus accumbens and prefrontal cortex following repeated treatment with amphetamine or cocaine. *The European journal of neuroscience* 1999; **11**(5)**:** 1598-1604.

33. Young EJ, Blouin AM, Briggs SB, Sillivan SE, Lin L, Cameron MD *et al.* Nonmuscle myosin IIB as a therapeutic target for the prevention of relapse to methamphetamine use. *Mol Psychiatry* 2016; **21**(5)**:** 615-623.

34. Benavides DR, Quinn JJ, Zhong P, Hawasli AH, DiLeone RJ, Kansy JW *et al.* Cdk5 modulates cocaine reward, motivation, and striatal neuron excitability. *The Journal of neuroscience : the official journal of the Society for Neuroscience* 2007; **27**(47)**:** 12967-12976.

35. Kiraly DD, Ma XM, Mazzone CM, Xin X, Mains RE, Eipper BA. Behavioral and morphological responses to cocaine require kalirin7. *Biological psychiatry* 2010; **68**(3)**:** 249-255.

36. Pulipparacharuvil S, Renthal W, Hale CF, Taniguchi M, Xiao G, Kumar A *et al.* Cocaine regulates MEF2 to control synaptic and behavioral plasticity. *Neuron* 2008; **59**(4)**:** 621-633.

37. Weber A, Pennise CR, Fowler VM. Tropomodulin increases the critical concentration of barbed end-capped actin filaments by converting ADP.P(i)-actin to ADP-actin at all pointed filament ends. *The Journal of biological chemistry* 1999; **274**(49)**:** 34637-34645.

38. Fischer RS, Fowler VM. Tropomodulins: life at the slow end. *Trends Cell Biol* 2003; **13**(11)**:** 593-601.

39. Omotade OF, Rui Y, Lei W, Yu K, Hartzell HC, Fowler VM *et al.* Tropomodulin Isoform-Specific Regulation of Dendrite Development and Synapse Formation. *The Journal of Neuroscience* 2018.

40. Gray KT, Suchowerska AK, Bland T, Colpan M, Wayman G, Fath T *et al.* Tropomodulin isoforms utilize specific binding functions to modulate dendrite development. *Cytoskeleton (Hoboken)* 2016; **73**(6)**:** 316-328.

41. Sussman MA, Sakhi S, Tocco G, Najm I, Baudry M, Kedes L *et al.* Neural tropomodulin: developmental expression and effect of seizure activity. *Brain research Developmental brain research* 1994; **80**(1-2)**:** 45-53.

42. Watakabe A, Kobayashi R, Helfman DM. N-tropomodulin: a novel isoform of tropomodulin identified as the major binding protein to brain tropomyosin. *Journal of cell science* 1996; **109 (Pt 9):** 2299-2310.

43. Yamashiro S, Speicher KD, Speicher DW, Fowler VM. Mammalian tropomodulins nucleate actin polymerization via their actin monomer binding and filament pointed end-capping activities. *The Journal of biological chemistry* 2010; **285**(43)**:** 33265-33280.

44. Davies G, Lam M, Harris SE, Trampush JW, Luciano M, Hill WD *et al.* Study of 300,486 individuals identifies 148 independent genetic loci influencing general cognitive function. *Nature communications* 2018; **9**(1)**:** 2098.

45. Hill WD, Marioni RE, Maghzian O, Ritchie SJ, Hagenaars SP, McIntosh AM *et al.* A combined analysis of genetically correlated traits identifies 187 loci and a role for neurogenesis and myelination in intelligence. *Mol Psychiatry* 2019; **24**(2)**:** 169-181.

46. Polimanti R, Meda SA, Pearlson GD, Zhao H, Sherva R, Farrer LA *et al.* S100A10 identified in a genome-wide gene x cannabis dependence interaction analysis of risky sexual behaviours. *J Psychiatry Neurosci* 2017; **42**(4)**:** 252-261.

47. Iwazaki T, McGregor IS, Matsumoto I. Protein expression profile in the striatum of acute methamphetamine-treated rats. *Brain Res* 2006; **1097**(1)**:** 19-25.

48. Zhang F, Chen L, Liu C, Qiu P, Wang A, Li L *et al.* Up-regulation of protein tyrosine nitration in methamphetamine-induced neurotoxicity through DDAH/ADMA/NOS pathway. *Neurochem Int* 2013; **62**(8)**:** 1055-1064.

49. Zhu L, Li J, Dong N, Guan F, Liu Y, Ma D *et al.* mRNA changes in nucleus accumbens related to methamphetamine addiction in mice. *Sci Rep* 2016; **6:** 36993.

50. Lesscher HM, Houthuijzen JM, Groot Koerkamp MJ, Holstege FC, Vanderschuren LJ. Amygdala 14-3-3zeta as a novel modulator of escalating alcohol intake in mice. *PloS one* 2012; **7**(5)**:** e37999.

51. Oliver RJ, Brigman JL, Bolognani F, Allan AM, Neisewander JL, Perrone-Bizzozero NI. Neuronal RNA-binding protein HuD regulates addiction-related gene expression and behavior. *Genes Brain Behav* 2018; **17**(4)**:** e12454.

52. Tapocik JD, Luu TV, Mayo CL, Wang BD, Doyle E, Lee AD *et al.* Neuroplasticity, axonal guidance and micro-RNA genes are associated with morphine self-administration behavior. *Addict Biol* 2013; **18**(3)**:** 480-495.

53. Li CY, Mao X, Wei L. Genes and (common) pathways underlying drug addiction. *PLoS Comput Biol* 2008; **4**(1)**:** e2.

54. Kumar V, Kim K, Joseph C, Thomas LC, Hong H, Takahashi JS. Second-generation high-throughput forward genetic screen in mice to isolate subtle behavioral mutants. *Proceedings of the National Academy of Sciences* 2011; **108**(Supplement 3)**:** 15557.

55. Dickson PE, Rogers TD, Lester DB, Miller MM, Matta SG, Chesler EJ *et al.* Genotype-dependent effects of adolescent nicotine exposure on dopamine functional dynamics in the nucleus accumbens shell in male and female mice: a potential mechanism underlying the gateway effect of nicotine. *Psychopharmacology* 2011; **215**(4)**:** 631-642.

56. Eagle AL, Gajewski PA, Yang M, Kechner ME, Al Masraf BS, Kennedy PJ *et al.* Experience-Dependent Induction of Hippocampal DeltaFosB Controls Learning. *The Journal of neuroscience : the official journal of the Society for Neuroscience* 2015; **35**(40)**:** 13773-13783.

57. de Guzman AE, Wong MD, Gleave JA, Nieman BJ. Variations in post-perfusion immersion fixation and storage alter MRI measurements of mouse brain morphometry. *NeuroImage* 2016; **142:** 687-695.

58. Spencer Noakes TL, Henkelman RM, Nieman BJ. Partitioning k-space for cylindrical three-dimensional rapid acquisition with relaxation enhancement imaging in the mouse brain. *NMR in biomedicine* 2017; **30**(11).

59. Friedel M, van Eede MC, Pipitone J, Chakravarty MM, Lerch JP. Pydpiper: a flexible toolkit for constructing novel registration pipelines. *Frontiers in neuroinformatics* 2014; **8:** 67.

60. Dorr AE, Lerch JP, Spring S, Kabani N, Henkelman RM. High resolution three-dimensional brain atlas using an average magnetic resonance image of 40 adult C57Bl/6J mice. *NeuroImage* 2008; **42**(1)**:** 60-69.

61. Benjamini Y, Hochberg Y. Controlling the False Discovery Rate: A Practical and Powerful Approach to Multiple Testing. *Journal of the Royal Statistical Society Series B (Methodological)* 1995; **57**(1)**:** 289-300.

62. Lerch JP, Gazdzinski L, Germann J, Sled JG, Henkelman RM, Nieman BJ. Wanted dead or alive? The tradeoff between in-vivo versus ex-vivo MR brain imaging in the mouse. *Frontiers in neuroinformatics* 2012; **6:** 6.

63. Tsai NP, Wilkerson JR, Guo W, Maksimova MA, DeMartino GN, Cowan CW *et al.* Multiple autism-linked genes mediate synapse elimination via proteasomal degradation of a synaptic scaffold PSD-95. *Cell* 2012; **151**(7)**:** 1581-1594.

64. Jewett KA, Lee KY, Eagleman DE, Soriano S, Tsai N-P. Dysregulation and restoration of homeostatic network plasticity in fragile X syndrome mice. *Neuropharmacology* 2018; **138:** 182-192.

65. Zhang ZW. Maturation of layer V pyramidal neurons in the rat prefrontal cortex: intrinsic properties and synaptic function. *Journal of neurophysiology* 2004; **91**(3)**:** 1171-1182.

66. Zhang ZW, Arsenault D. Gain modulation by serotonin in pyramidal neurones of the rat prefrontal cortex. *The Journal of physiology* 2005; **566**(Pt 2)**:** 379-394.

67. Badiani A, Robinson TE. Drug-induced neurobehavioral plasticity: the role of environmental context. *Behavioural pharmacology* 2004; **15**(5-6)**:** 327-339.

68. Zhang W, Peterson M, Beyer B, Frankel WN, Zhang Z-w. Loss of MeCP2 From Forebrain Excitatory Neurons Leads to Cortical Hyperexcitation and Seizures. *The Journal of Neuroscience* 2014; **34**(7)**:** 2754.

69. Ball SA, Kranzler HR, Tennen H, Poling JC, Rounsaville BJ. Personality disorder and dimension differences between type A and type B substance abusers. *Journal of personality disorders* 1998; **12**(1)**:** 1-12.

70. Brady KT, Haynes LF, Hartwell KJ, Killeen TK. Substance use disorders and anxiety: a treatment challenge for social workers. *Social work in public health* 2013; **28**(3-4)**:** 407-423.

71. Franques P, Auriacombe M, Piquemal E, Verger M, Brisseau-Gimenez S, Grabot D *et al.* Sensation seeking as a common factor in opioid dependent subjects and high risk sport practicing subjects. A cross sectional study. *Drug and alcohol dependence* 2003; **69**(2)**:** 121-126.

72. Dickson PE, Ndukum J, Wilcox T, Clark J, Roy B, Zhang L *et al.* Association of novelty-related behaviors and intravenous cocaine self-administration in Diversity Outbred mice. *Psychopharmacology* 2015; **232**(6)**:** 1011-1024.

73. Molander AC, Mar A, Norbury A, Steventon S, Moreno M, Caprioli D *et al.* High impulsivity predicting vulnerability to cocaine addiction in rats: some relationship with novelty preference but not novelty reactivity, anxiety or stress. *Psychopharmacology* 2011; **215**(4)**:** 721-731.

74. Lever C, Burton S, O'Keefe J. Rearing on hind legs, environmental novelty, and the hippocampal formation. *Reviews in the neurosciences* 2006; **17**(1-2)**:** 111-133.

75. Hascoet M, Bourin M, Nic Dhonnchadha BA. The mouse light-dark paradigm: a review. *Progress in neuro-psychopharmacology & biological psychiatry* 2001; **25**(1)**:** 141-166.

76. Robinson TE, Berridge KC. Addiction. *Annual review of psychology* 2003; **54:** 25-53.

77. Vanderschuren LJ, Kalivas PW. Alterations in dopaminergic and glutamatergic transmission in the induction and expression of behavioral sensitization: a critical review of preclinical studies. *Psychopharmacology* 2000; **151**(2-3)**:** 99-120.

78. Phillips TJ. Behavior genetics of drug sensitization. *Critical reviews in neurobiology* 1997; **11**(1)**:** 21-33.

79. Steketee JD, Kalivas PW. Drug wanting: behavioral sensitization and relapse to drug-seeking behavior. *Pharmacological reviews* 2011; **63**(2)**:** 348-365.

80. Bolivar VJ. Intrasession and intersession habituation in mice: from inbred strain variability to linkage analysis. *Neurobiology of learning and memory* 2009; **92**(2)**:** 206-214.

81. Belin-Rauscent A, Fouyssac M, Bonci A, Belin D. How Preclinical Models Evolved to Resemble the Diagnostic Criteria of Drug Addiction. *Biological psychiatry* 2016; **79**(1)**:** 39-46.

82. Benuck M, Lajtha A, Reith ME. Pharmacokinetics of systemically administered cocaine and locomotor stimulation in mice. *The Journal of pharmacology and experimental therapeutics* 1987; **243**(1)**:** 144-149.

83. Bailey SA, Zidell RH, Perry RW. Relationships between organ weight and body/brain weight in the rat: what is the best analytical endpoint? *Toxicologic pathology* 2004; **32**(4)**:** 448-466.

84. Agrawal HC, Davis JM, Himwich WA. Developmental changes in mouse brain: weight, water content and free amino acids. *Journal of neurochemistry* 1968; **15**(9)**:** 917-923.

85. Parikshak NN, Gandal MJ, Geschwind DH. Systems biology and gene networks in neurodevelopmental and neurodegenerative disorders. *Nature reviews Genetics* 2015; **16**(8)**:** 441-458.

86. Srinivasan K, Friedman BA, Larson JL, Lauffer BE, Goldstein LD, Appling LL *et al.* Untangling the brain's neuroinflammatory and neurodegenerative transcriptional responses. *Nature communications* 2016; **7:** 11295.

87. Torre D, Lachmann A, Ma'ayan A. BioJupies: Automated Generation of Interactive Notebooks for RNA-Seq Data Analysis in the Cloud. *Cell systems* 2018; **7**(5)**:** 556-561.e553.

88. Gray KT, Kostyukova AS, Fath T. Actin regulation by tropomodulin and tropomyosin in neuronal morphogenesis and function. *Mol Cell Neurosci* 2017; **84:** 48-57.

89. Cox PR, Zoghbi HY. Sequencing, expression analysis, and mapping of three unique human tropomodulin genes and their mouse orthologs. *Genomics* 2000; **63**(1)**:** 97-107.

90. Kauer JA, Malenka RC. Synaptic plasticity and addiction. *Nature reviews Neuroscience* 2007; **8**(11)**:** 844-858.

91. Malenka RC, Nicoll RA. Long-term potentiation--a decade of progress? *Science (New York, NY)* 1999; **285**(5435)**:** 1870-1874.

92. Robinson TE, Kolb B. Structural plasticity associated with exposure to drugs of abuse. *Neuropharmacology* 2004; **47 Suppl 1:** 33-46.

93. Ishikawa M, Otaka M, Neumann PA, Wang Z, Cook JM, Schluter OM *et al.* Exposure to cocaine regulates inhibitory synaptic transmission from the ventral tegmental area to the nucleus accumbens. *The Journal of physiology* 2013; **591**(19)**:** 4827-4841.

94. Li Z, Chen Z, Fan G, Li A, Yuan J, Xu T. Cell-Type-Specific Afferent Innervation of the Nucleus Accumbens Core and Shell. *Frontiers in Neuroanatomy* 2018; **12**(84).

95. Kilman V, van Rossum MC, Turrigiano GG. Activity deprivation reduces miniature IPSC amplitude by decreasing the number of postsynaptic GABA(A) receptors clustered at neocortical synapses. *The Journal of neuroscience : the official journal of the Society for Neuroscience* 2002; **22**(4)**:** 1328-1337.

96. Hu Z, Yu D, Gu QH, Yang Y, Tu K, Zhu J *et al.* miR-191 and miR-135 are required for long-lasting spine remodelling associated with synaptic long-term depression. *Nature communications* 2014; **5:** 3263.

97. Ly C, Greb AC, Cameron LP, Wong JM, Barragan EV, Wilson PC *et al.* Psychedelics Promote Structural and Functional Neural Plasticity. *Cell reports* 2018; **23**(11)**:** 3170-3182.

98. Cahill ME, Walker DM, Gancarz AM, Wang ZJ, Lardner CK, Bagot RC *et al.* The dendritic spine morphogenic effects of repeated cocaine use occur through the regulation of serum response factor signaling. *Molecular Psychiatry* 2017; **23:** 1474.

99. Dos Santos M, Salery M, Forget B, Garcia Perez MA, Betuing S, Boudier T *et al.* Rapid Synaptogenesis in the Nucleus Accumbens Is Induced by a Single Cocaine Administration and Stabilized by Mitogen-Activated Protein Kinase Interacting Kinase-1 Activity. *Biological psychiatry* 2017; **82**(11)**:** 806-818.

100. Blanchard MM, Mendelsohn D, Stamp JA. The HR/LR model: Further evidence as an animal model of sensation seeking. *Neuroscience and biobehavioral reviews* 2009; **33**(7)**:** 1145-1154.

101. Davis BA, Clinton SM, Akil H, Becker JB. The effects of novelty-seeking phenotypes and sex differences on acquisition of cocaine self-administration in selectively bred High-Responder and Low-Responder rats. *Pharmacology, biochemistry, and behavior* 2008; **90**(3)**:** 331-338.

102. Dellu F, Piazza PV, Mayo W, Le Moal M, Simon H. Novelty-seeking in rats--biobehavioral characteristics and possible relationship with the sensation-seeking trait in man. *Neuropsychobiology* 1996; **34**(3)**:** 136-145.

103. Kourrich S, Calu DJ, Bonci A. Intrinsic plasticity: an emerging player in addiction. *Nature reviews Neuroscience* 2015; **16**(3)**:** 173-184.

104. Chang JY, Sawyer SF, Paris JM, Kirillov A, Woodward DJ. Single neuronal responses in medial prefrontal cortex during cocaine self-administration in freely moving rats. *Synapse (New York, NY)* 1997; **26**(1)**:** 22-35.

105. Sun W, Rebec GV. Repeated Cocaine Self-Administration Alters Processing of Cocaine-Related Information in Rat Prefrontal Cortex. *The Journal of Neuroscience* 2006; **26**(30)**:** 8004.

106. Bolloni C, Panella R, Pedetti M, Frascella AG, Gambelunghe C, Piccoli T *et al.* Bilateral Transcranial Magnetic Stimulation of the Prefrontal Cortex Reduces Cocaine Intake: A Pilot Study. *Frontiers in psychiatry* 2016; **7:** 133.

107. Rapinesi C, Del Casale A, Di Pietro S, Ferri VR, Piacentino D, Sani G *et al.* Add-on high frequency deep transcranial magnetic stimulation (dTMS) to bilateral prefrontal cortex reduces cocaine craving in patients with cocaine use disorder. *Neuroscience letters* 2016; **629:** 43-47.

108. Terraneo A, Leggio L, Saladini M, Ermani M, Bonci A, Gallimberti L. Transcranial magnetic stimulation of dorsolateral prefrontal cortex reduces cocaine use: A pilot study. *European neuropsychopharmacology : the journal of the European College of Neuropsychopharmacology* 2016; **26**(1)**:** 37-44.

109. Kourrich S, Rothwell PE, Klug JR, Thomas MJ. Cocaine Experience Controls Bidirectional Synaptic Plasticity in the Nucleus Accumbens. *The Journal of Neuroscience* 2007; **27**(30)**:** 7921.

110. Kim J, Park B-H, Lee JH, Park SK, Kim J-H. Cell Type-Specific Alterations in the Nucleus Accumbens by Repeated Exposures to Cocaine. *Biological psychiatry* 2011; **69**(11)**:** 1026-1034.

111. Bateup HS, Santini E, Shen W, Birnbaum S, Valjent E, Surmeier DJ *et al.* Distinct subclasses of medium spiny neurons differentially regulate striatal motor behaviors. *Proc Natl Acad Sci U S A* 2010; **107**(33)**:** 14845-14850.

112. Brincat SL, Miller EK. Frequency-specific hippocampal-prefrontal interactions during associative learning. *Nature neuroscience* 2015; **18**(4)**:** 576-581.

113. Day JJ, Roitman MF, Wightman RM, Carelli RM. Associative learning mediates dynamic shifts in dopamine signaling in the nucleus accumbens. *Nature neuroscience* 2007; **10**(8)**:** 1020-1028.

114. Lim KO, Wozniak JR, Mueller BA, Franc DT, Specker SM, Rodriguez CP *et al.* Brain macrostructural and microstructural abnormalities in cocaine dependence. *Drug and alcohol dependence* 2008; **92**(1-3)**:** 164-172.

115. Moeller FG, Hasan KM, Steinberg JL, Kramer LA, Dougherty DM, Santos RM *et al.* Reduced anterior corpus callosum white matter integrity is related to increased impulsivity and reduced discriminability in cocaine-dependent subjects: diffusion tensor imaging. *Neuropsychopharmacology : official publication of the American College of Neuropsychopharmacology* 2005; **30**(3)**:** 610-617.

116. Garza-Villarreal EA, Chakravarty MM, Hansen B, Eskildsen SF, Devenyi GA, Castillo-Padilla D *et al.* The effect of crack cocaine addiction and age on the microstructure and morphology of the human striatum and thalamus using shape analysis and fast diffusion kurtosis imaging. *Translational psychiatry* 2017; **7**(5)**:** e1122.

117. Korponay C, Kosson DS, Decety J, Kiehl KA, Koenigs M. Brain Volume Correlates with Duration of Abstinence from Substance Abuse in a Region-Specific and Substance-Specific Manner. *Biological psychiatry Cognitive neuroscience and neuroimaging* 2017; **2**(7)**:** 626-635.

118. Fath T, Fischer RS, Dehmelt L, Halpain S, Fowler VM. Tropomodulins are negative regulators of neurite outgrowth. *Eur J Cell Biol* 2011; **90**(4)**:** 291-300.

119. Briggs SB, Blouin AM, Young EJ, Rumbaugh G, Miller CA. Memory disrupting effects of nonmuscle myosin II inhibition depend on the class of abused drug and brain region. *Learning & memory (Cold Spring Harbor, NY)* 2017; **24**(2)**:** 70-75.

120. Briggs SB, Hafenbreidel M, Young EJ, Rumbaugh G, Miller CA. The role of nonmuscle myosin II in polydrug memories and memory reconsolidation. *Learning & memory (Cold Spring Harbor, NY)* 2018; **25**(9)**:** 391-398.

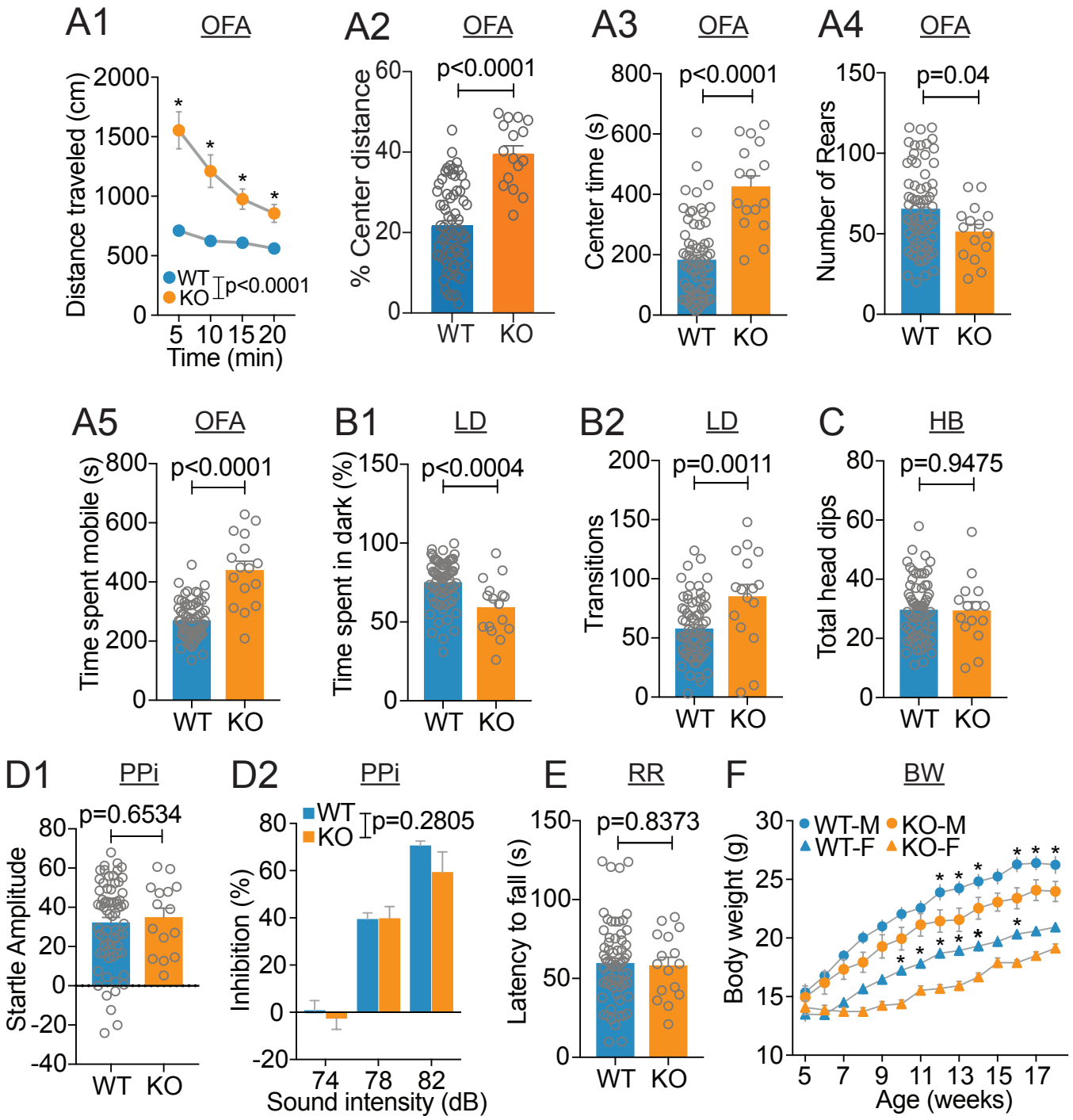
A1
OFA
Distance traveled (cm)
2000
1500
1000
500
0
WT
KO
p<0.0001
5 10 15 20
Time (min)
A2
OFA
% Center distance
60
40
20
0
p<0.0001
WT KO
A3
OFA
Center time (s)
800
600
400
200
0
p<0.0001
WT KO
A4
OFA
Number of Rears
150
100
50
0
p=0.04
WT KO
A5
OFA
Time spent mobile (s)
800
600
400
200
0
p<0.0001
WT KO
B1
LD
Time spent in dark (%)
150
100
50
0
p<0.0004
WT KO
B2
LD
Transitions
200
150
100
50
0
p=0.0011
WT KO
C
HB
Total head dips
80
60
40
20
0
p=0.9475
WT KO
D1
PPi
Startle Amplitude
80
60
40
20
0
-20
-40
p=0.6534
WT KO
D2
PPi
Inhibition (%)
80
60
40
20
0
-20
WT
KO
p=0.2805
74 78 82
Sound intensity (dB)
E
RR
Latency to fall (s)
150
100
50
0
p=0.8373
WT KO
F
BW
Body weight (g)
30
25
20
15
10
WT-M
KO-M
WT-F
KO-F
5 7 9 11 13 15 17
Age (weeks)

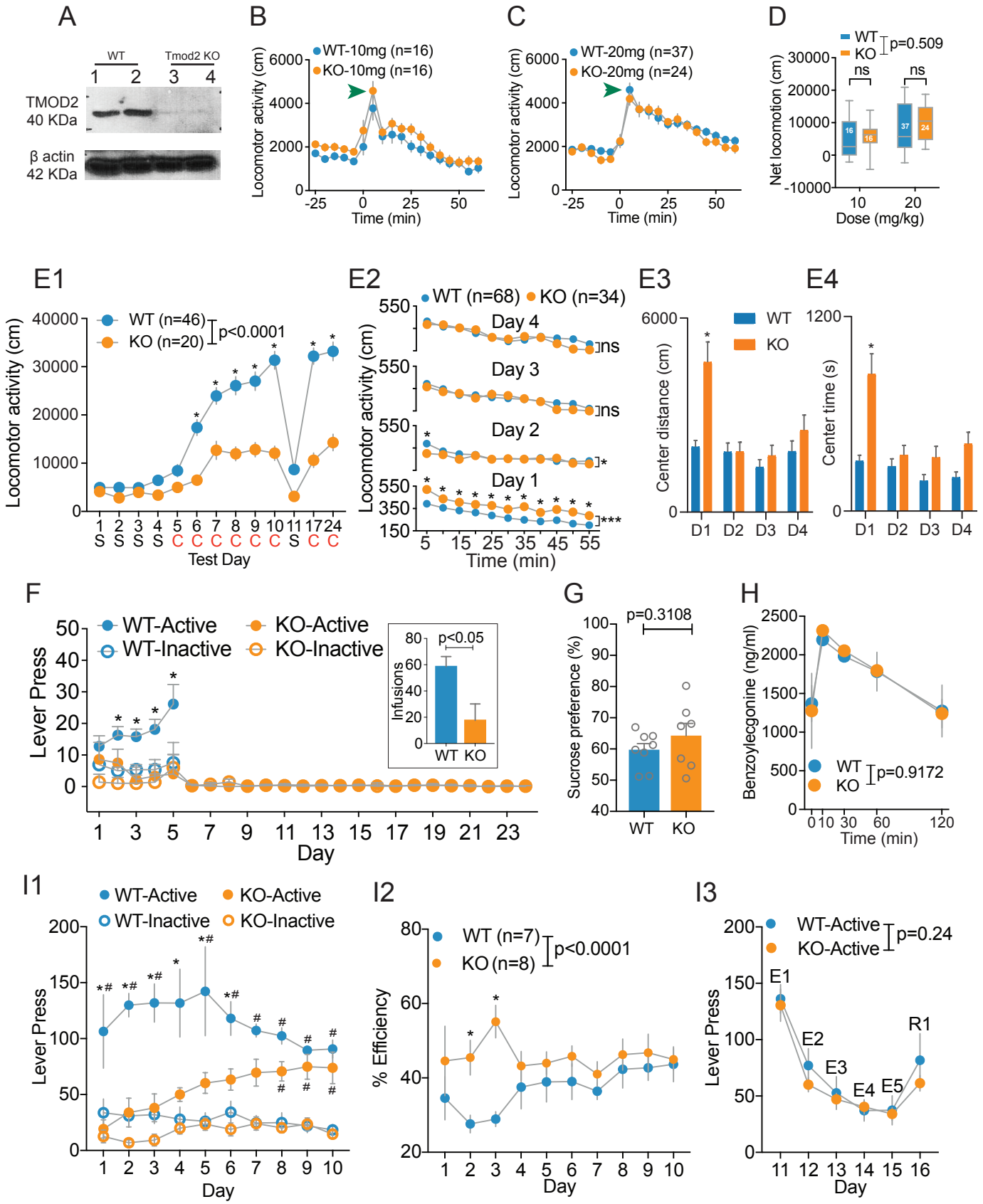
A
WT
Tmod2 KO
1 2 3 4
TMOD2
40 KDa
β actin
42 KDa
B
WT-10mg (n=16)
KO-10mg (n=16)
Locomotor activity (cm)
Time (min)
C
WT-20mg (n=37)
KO-20mg (n=24)
Locomotor activity (cm)
Time (min)
D
WT
KO
p=0.509
ns
ns
Net locomotion (cm)
Dose (mg/kg)
E1
WT (n=46)
KO (n=20)
p<0.0001
Locomotor activity (cm)
Test Day
E2
WT (n=68)
KO (n=34)
Day 4
Day 3
Day 2
Day 1
ns
ns
*
***
Locomotor activity (cm)
Time (min)
E3
WT
KO
Center distance (cm)
D1 D2 D3 D4
E4
Center time (s)
D1 D2 D3 D4
F
WT-Active
WT-Inactive
KO-Active
KO-Inactive
Lever Press
Day
p<0.05
Infusions
WT KO
G
p=0.3108
Sucrose preference (%)
WT KO
H
WT
KO
p=0.9172
Benzoylecgonine (ng/ml)
Time (min)
I1
WT-Active
WT-Inactive
KO-Active
KO-Inactive
Lever Press
Day
I2
WT (n=7)
KO (n=8)
p<0.0001
% Efficiency
Day
I3
WT-Active
KO-Active
p=0.24
E1
E2
E3
E4
E5
R1
Lever Press
Day

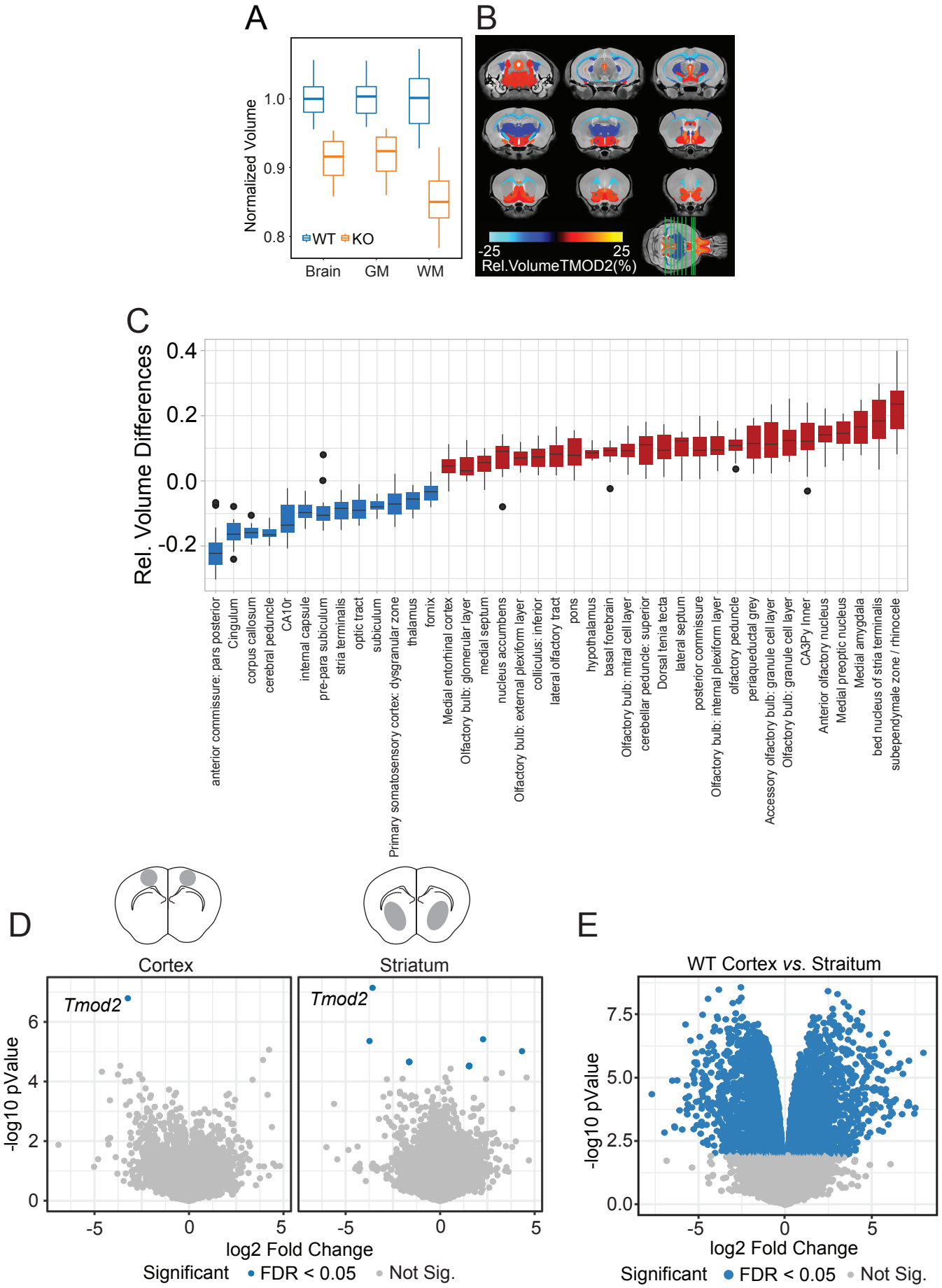
A
Normalized Volume
1.0
0.9
0.8
WT
KO
Brain
GM
WM
B
-25
25
Rel.VolumeTMOD2(%)
C
Rel. Volume Differences
0.4
0.2
0.0
-0.2
anterior commissure: pars posterior
Cingulum
corpus callosum
cerebral peduncle
CA1or
internal capsule
pre-para subiculum
stria terminalis
optic tract
subiculum
Primary somatosensory cortex: dysgranular zone
thalamus
fornix
Medial entorhinal cortex
Olfactory bulb: glomerular layer
medial septum
nucleus accumbens
Olfactory bulb: external plexiform layer
colliculus: inferior
lateral olfactory tract
pons
hypothalamus
basal forebrain
Olfactory bulb: mitral cell layer
cerebellar peduncle: superior
Dorsal tenia tecta
lateral septum
posterior commissure
Olfactory bulb: internal plexiform layer
olfactory peduncle
periaqueductal grey
Accessory olfactory bulb: granule cell layer
Olfactory bulb: granule cell layer
CA3Py Inner
Anterior olfactory nucleus
Medial preoptic nucleus
Medial amygdala
bed nucleus of stria terminalis
subependymale zone / rhinocele
D
Cortex
Striatum
Tmod2
Tmod2
-log10 pValue
6
4
2
0
-5
0
5
log2 Fold Change
Significant
FDR < 0.05
Not Sig.
E
WT Cortex vs. Straitum
-log10 pValue
7.5
5.0
2.5
0.0
-5
0
5
log2 Fold Change
Significant
FDR < 0.05
Not Sig.

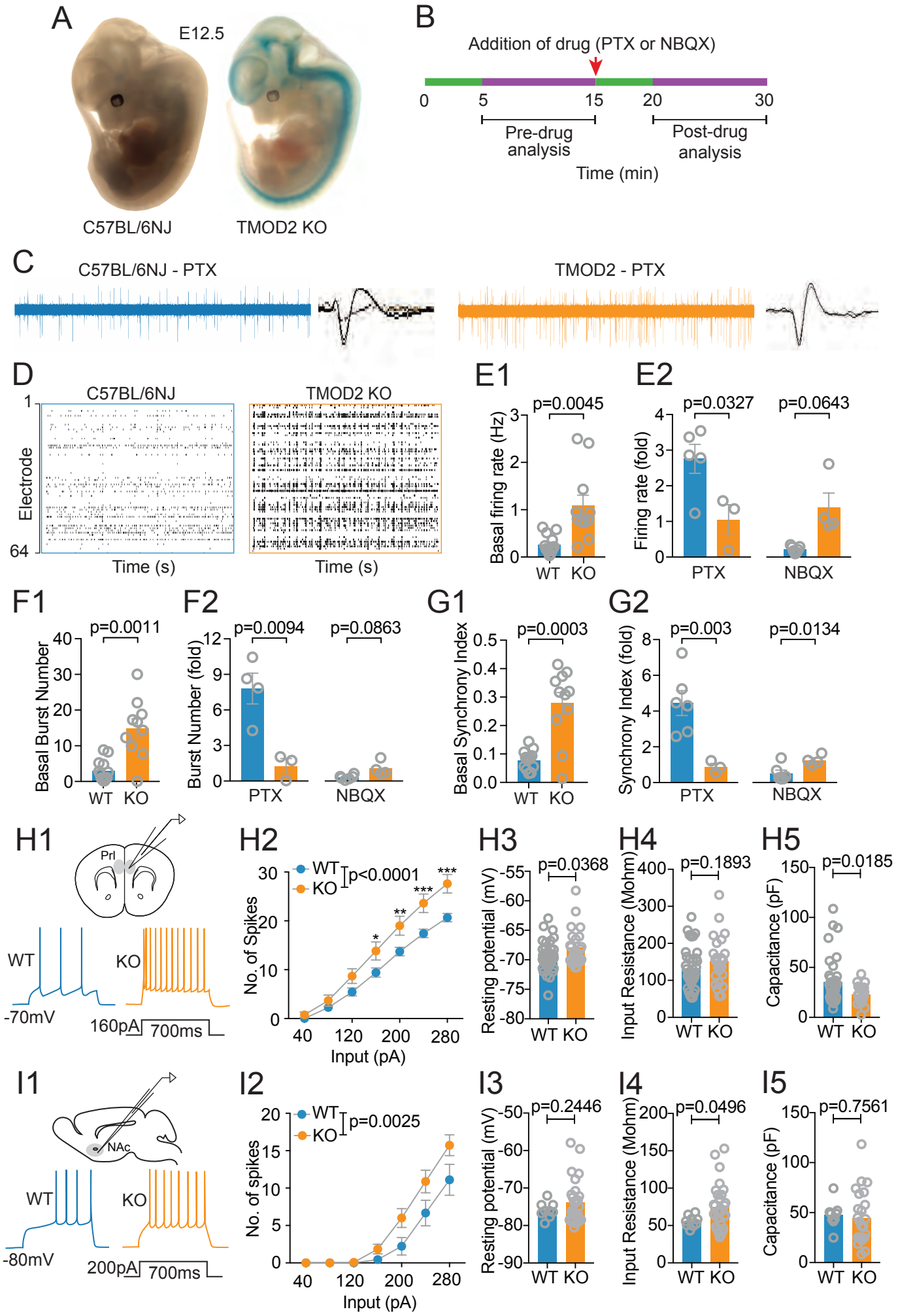
A
E12.5
C57BL/6NJ
TMOD2 KO
B
Addition of drug (PTX or NBQX)
0
5
15
20
30
Pre-drug analysis
Post-drug analysis
Time (min)
C
C57BL/6NJ - PTX
TMOD2 - PTX
D
C57BL/6NJ
TMOD2 KO
Electrode
1
64
Time (s)
Time (s)
E1
Basal firing rate (Hz)
p=0.0045
WT KO
E2
Firing rate (fold)
p=0.0327
p=0.0643
PTX
NBQX
F1
Basal Burst Number
p=0.0011
WT KO
F2
Burst Number (fold)
p=0.0094
p=0.0863
PTX
NBQX
G1
Basal Synchrony Index
p=0.0003
WT KO
G2
Synchrony Index (fold)
p=0.003
p=0.0134
PTX
NBQX
H1
Prl
WT
KO
-70mV
160pA
700ms
H2
WT
KO
p<0.0001
No. of Spikes
Input (pA)
H3
Resting potential (mV)
p=0.0368
WT KO
H4
Input Resistance (Mohm)
p=0.1893
WT KO
H5
Capacitance (pF)
p=0.0185
WT KO
I1
NAc
WT
KO
-80mV
200pA
700ms
I2
WT
KO
p=0.0025
No. of spikes
Input (pA)
I3
Resting potential (mV)
p=0.2446
WT KO
I4
Input Resistance (Mohm)
p=0.0496
WT KO
I5
Capacitance (pF)
p=0.7561
WT KO

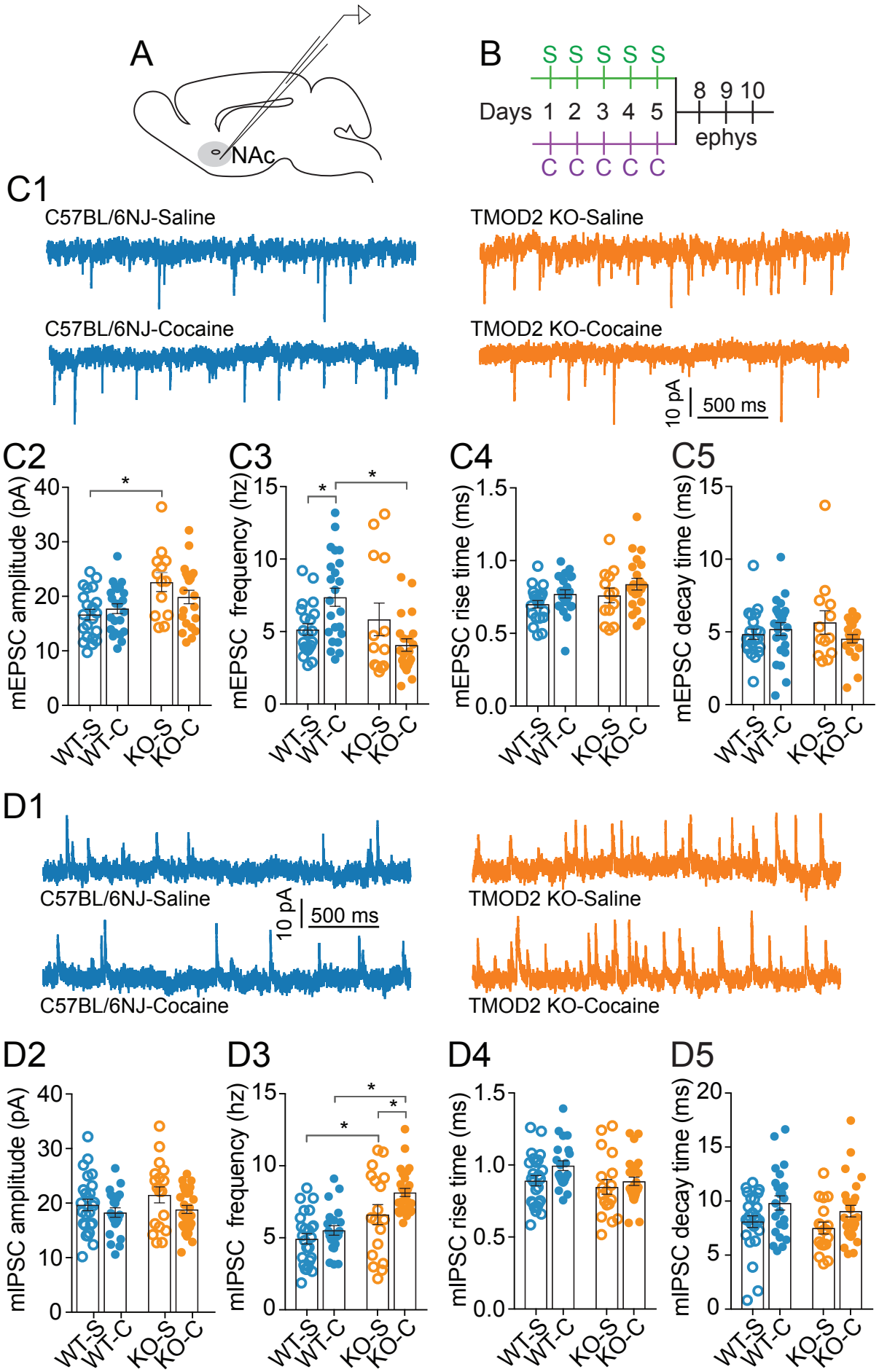
A
NAc
B
S S S S S
Days 1 2 3 4 5
8 9 10
ephys
C C C C C
C1
C57BL/6NJ-Saline
TMOD2 KO-Saline
C57BL/6NJ-Cocaine
TMOD2 KO-Cocaine
10 pA
500 ms
C2
mEPSC amplitude (pA)
C3
mEPSC frequency (hz)
C4
mEPSC rise time (ms)
C5
mEPSC decay time (ms)
WT-S
WT-C
KO-S
KO-C
D1
C57BL/6NJ-Saline
TMOD2 KO-Saline
C57BL/6NJ-Cocaine
TMOD2 KO-Cocaine
10 pA
500 ms
D2
mIPSC amplitude (pA)
D3
mIPSC frequency (hz)
D4
mIPSC rise time (ms)
D5
mIPSC decay time (ms)